國立臺灣大學生命科學院植物科學研究所

博士論文

Institute of Plant Biology

College of Life Science

National Taiwan University

Doctoral Dissertation

阿拉伯芥麩胺基硫轉移酶 AtGSTU17 突變株耐旱及耐鹽性狀為麩胺基與離層酸共同作用之結果

Drought and Salt Stress Tolerance of Arabidopsis Glutathione S-Transferase U17 Knockout Mutant are Attributed to the Combined Effect of Glutathione and Abscisic Acid

陳瑞宏

Jui-Hung Chen

指導教授：林讚標 博士

Advisor: Tsan-Piao Lin, Ph.D.

中華民國一百年十二月

December, 2011

國立臺灣大學博士學位論文

口試委員會審定書

阿拉伯芥麩氨基硫轉移酶 AtGSTU17 突變株耐旱及耐鹽性狀為麩氨基與離層酸共同作用之結果

Drought and Salt Stress Tolerance of Arabidopsis Glutathione S-Transferase U17 Knockout Mutant are Attributed to the Combined Effect of Glutathione and Abscisic Acid

本論文係陳瑞宏君 (D92B42005) 在國立臺灣大學植物科學所完成之博士學位論文，於民國一百年十二月三十日承下列考試委員審查通過及口試及格，特此證明

口試委員：

臺灣大學植物科學所
林讚標 教授 林讚標

臺灣大學植物科學所
鄭石通 教授 鄭石通

臺灣大學植物科學所
謝旭亮 副教授 謝旭亮

臺灣大學農業化學系
洪傳揚 副教授 洪傳揚

成功大學生物多樣性研究所
陳虹樺 教授 陳虹樺

中央研究院農業生物科技研究中心
葉國楨 副研究員 葉國楨

中文摘要

麩胺基硫轉移酶 (glutathione s-transferases, GSTs) 在氧化逆境代謝中扮演一個相當重要的角色，但對於這類基因在植物體內所扮演的個別功能卻所知有限。在整個 GST 基因家族中 *GLUTATHIONE S-TRANSFERASE U17* (*AtGSTU17*, At1g10370) 曾有被報導其參與了光的傳導訊息調控；經由與 phyA 的交互作用，影響了植物體內的 GSH 含量，進一步影響了植物的生長發育。

本篇論文提供進一步的研究證據顯示 *AtGSTU17* 在乾旱及鹽分逆境下扮演一個重要的負調控角色。阿拉伯芥的 *atgstu17* 突變株比野生型更爲耐旱及耐鹽。生理分析顯示 *atgstu17* 突變株的植物體累積了較高含量的 GSH 與 ABA，同時在發芽時期對於 ABA 較不敏感，葉片的氣孔孔徑較小，較低的水分蒸發速率，根系發育更爲茂盛以及較長的營養生長期等生理性狀。

爲了釐清 *atgstu17* 突變株累積的 ABA 是否是因爲 GSH 含量升高引起，我們對野生型澆灌 GSH 溶液進行研究。結果發現澆灌 GSH 溶液的野生型，其 ABA 含量較未澆灌 GSH 的植株高，同時顯現 *atgstu17* 突變株的生理性狀，如開花延遲，根部發育，較爲耐鹽與耐旱等。進一步研究 *atgstu17* 突變株是否是因爲 GSH 與 ABA 累積影響而產生了上述的生理性狀。我們將 *atgstu17* 突變株種植在 L-buthionine-(*S*,*R*)-sulfoximine (BSO)溶液中。BSO 是一種可以抑制植物的 GSH 生合成的專一性藥劑。當 *atgstu17* 突變株的 GSH 含量受到 BSO 抑制減少到與野生型相同的含量時，觀察其性狀與生理反應，如根系，開花時間與對於鹽分與乾旱的耐受性等，顯示與野生型類似。由以上實驗結果可以得到一個結論，*atgstu17* 突變株的外表性狀是由於其植物體內含有較高的 GSH 與 ABA 所共同作用而產生的結果。同時經由 DNA 微陣列 (microarray) 的資料顯示許多與生長或逆境相關的轉錄調控基因受到 AtGSTU17 的影響而改變表現。綜合以上實驗資料結果，我們推測 AtGSTU17 扮演了植物逆境訊息傳導反應的負調控功能。

ABSTRACT

Although glutathione S-transferases (GSTs) are thought to play major roles in oxidative stress metabolism, little is known about the regulatory functions of GSTs. We have reported that *GLUTATHIONE S-TRANSFERASE U17* (*AtGSTU17*, At1g10370) participates in light signaling and might modulate various aspects of development by affecting glutathione (GSH) pools via a coordinated regulation with phyA. Here we provided further evidence to support a negative role of *AtGSTU17* in drought and salt stress tolerance.

When *AtGSTU17* was mutated, plants were more tolerant to drought and salt stresses compared to wild-type (WT, Col-0) plants. In addition, *atgstu17* accumulated higher level of GSH and abscisic acid (ABA), and exhibited hyposensitivity to ABA during seed germination, smaller stomatal apertures, a lower transpiration rate, better development of primary and lateral root systems, and longer vegetative growth.

To explore how *atgstu17* accumulated higher ABA content, we grew WT in the solution containing GSH and found that plants accumulated ABA to a higher extent than plants grown in the absence of GSH, and exhibited the *atgstu17* phenotypes. WT plants treated with GSH also demonstrated more tolerant to drought and salt stresses. Furthermore, the effect of GSH on root patterning and drought tolerance was confirmed by growing the *atgstu17* in solution containing L-buthionine-(*S*,*R*)-sulfoximine (BSO), a specific inhibitor of GSH biosynthesis.

In conclusion, the *atgstu17* phenotype can be explained by the combined effect of GSH and ABA. Microarray analysis provided evidence that expressions of many genes related to growth and stress inducible transcription factors altered in the *atgstu17* mutants. We propose a role of AtGSTU17 in adaptive responses to drought and salt stresses, by functioning as a negative component of stress-mediated signal

transduction pathways.

CONTENTS

INTRODUCTION

In both animals and plants, glutathione S-transferases (GSTs; EC 2.5.1.18) are induced by diverse environmental stimuli, with increased GST levels used to maintain cell redox homeostasis and protect organisms against oxidative stress. GSTs were proposed to afford protection under various stress conditions by detoxifying endogenous plant toxins that accumulate as a consequence of increased oxidative stress (Marrs, 1996). In plants, *GST* expression is induced by phytohormones, such as salicylic acid, ethylene, cytokinin, auxin, abscisic acid (ABA) (Marrs, 1996), methyl jasmonate (Moons, 2003) and brassinosteroid (Deng et al., 2010). It is obvious that GSTs are also stimulated by various stresses, such as pathogen infections, herbicide applications, hydrogen peroxide, ozone, 2,4-dichlorophenoxy-acetic acid (2,4-D), heavy metals, dehydration, senescence, wounding (Marrs, 1996), hypoxic stress, and salt (Moons, 2003), as well as different qualities of light (Loyall et al., 2000; Tepperman et al., 2001; Chen et al., 2007). Glutathione (GSH) is an essential thiol antioxidant as well as a scavenger of reactive electrophilic compounds, functioning with GSTs to detoxify a range of herbicides (Marrs and Walbot, 1997; Edwards et al., 2000), by tagging electrophilic compounds for removal during oxidative stress. Theoretically, GST activities catalyze the conjugation of electrophilic compounds to GSH and target them for storage in vacuoles or apoplast (Marrs, 1996). Some plant GSTs play direct roles in reducing oxidative damage (Cummins et al., 1999; Roxas et al., 2000) and enhancing tolerance to stresses (Edwards and Dixon, 2005).

The GST family of *Arabidopsis thaliana* contains 54 members belonging to seven distinct classes (Fig. S1) (Dixon et al., 2009). The plant-specific phi (GSTF) and tau (GSTU) classes are the largest, with 13 and 28 members, respectively. By applying a range of stress stimuli, with a focus on early changes in gene expressions, Sappl et al. (2009) indicated that individual GST genes have highly specific induction patterns, and they linked individual GSTs to particular stress stimuli. However, analysis of

metabolite pools of lines in which GSTF genes were silenced showed involvement in protecting plants against oxidation of the primary metabolism. There appears to be a high degree of functional redundancy within the GST family for protecting against oxidative stresses. So far no known specific functions were identified in plant development for most of the members in the large GST gene family indicates a challenge when studying the function of individual genes in response to a stress.

In addition to this well-documented catalytic function, GSTs also function as non-catalytic carrier proteins (Sheehan et al., 2001). Only limited reports revealed the endogenous function of GSTs. For example, At5g17200 (AtGSTF12, also referred to as TT19) is required for the vacuolar uptake of anthocyanins (Kitamura et al., 2004). Also, GSTs can serve as signaling molecules, and are involved in regulating chalcone synthase following exposure to UV light (Loyall et al., 2000), possibly due to redox-modulated mechanisms. Recently, At1g78730 (AtGSTU20) was demonstrated to physically interact with far-red insensitive 219 (FIN219) in response to light and to play a crucial signaling role in cell elongation and plant development (Chen et al., 2007).

Very little information is available on the involvement of GSTs in response to drought and salt stresses, although changes in the GSH pool, glutathione reductase and glutathione peroxidase activities in dehydrated plants were described (Loggini et al., 1999; Galle et al., 2009). Tobacco seedlings but not mature plants over-expressing a tobacco tau GST gene were more tolerant to low- and high-temperature stresses, and salt stress (Roxas et al., 2000). Tobacco plants overexpressing a tau class of the GST gene, *GsGST* from *Glycine soja* exhibited enhanced dehydration tolerance (Ji et al., 2010). However, no further study was provided to support a hypothesis of the regulatory role of this gene in drought-exposed plants.

Recent studies have shown that *AtGSTU17* transcripts were induced by FR light

irradiation and regulated by different photoreceptors, especially phyA. Its loss-of-function mutants resulted in a long-hypocotyl phenotype under FR light and delayed flowering under long-day conditions (Jiang et al., 2010). AtGSTU17 came to our attention because it was regulated by FIN219/JAR1 and rapidly increased with far-red (FR) light irradiation but was inhibited by a *phyA* mutation (Tepperman et al., 2001; Jiang et al., 2010). The full-length complementary DNA (cDNA) of *AtGSTU17* encodes a 227 amino acid protein. The recombinant proteins generated from an *Escherichia coli* expression system showed enzymatic activities to the substrates GSH and 1-chloro-2,4-dinitrobenzene (CDNB), which indicates that AtGSTU17 has high affinity to both substrates (Dixon et al., 2009; Jiang et al., 2010). Moreover, we found that AtGSTU17 participates in phyA-mediated photomorphogenesis, and integrates with various phytohormones to modulate GSH homeostasis in regulating Arabidopsis development (Jiang et al., 2010). Surprisingly, *atgstu17* plants exhibited robust root system development especially under stress conditions and lack of sensitivity to ABA-mediated inhibition of lateral root elongation. Our present data clearly elucidate AtGSTU17 functions in an undiscovered negative role of adaptation to drought and salt stresses, and the underlying mechanism of the *atgstu17* phenotypes can be explained by the synergic action of GSH and ABA which accumulated to a much higher levels than in WT plants. GSH in addition to ABA in protection of plant under drought and salt stress therefore are important for the survival and growth of eukaryotic organisms.

MATERIALS AND METHODS

Plant Material and Growth Conditions

Arabidopsis thaliana WT, transgenic plants, and T-DNA-tagged mutants used in this work were of the Col-0 ecotype. The mutant seeds with a T-DNA insertion in the *AtGSTU17* gene (Salk_139615 line for *atgstu17-1* and Salk_025503 for *atgstu17-2*) were obtained from the Arabidopsis Biological Resource Center. Vector construction and plant transformation for generating *AtGSTU17*-overexpressing lines were previously described (Jiang et al., 2010). For creating complementary lines, *35S:GSTU17OE-5/atgstu17-1* and *35S:GSTU17OE-3/atgstu17-2*, the plasmid originally used in the paper of Jiang et al. (2010) was applied.

Seeds were sown in a 2:2:1 mixture of vermiculite: perlite: and peat moss. Plants were placed at 4 ^{o}C for 3 days in the dark for stratification and then transferred to normal growth conditions. Plants were grown at 22 ^{o}C under long-day conditions (a 16-h light/8-h dark cycle). For *in vitro* culture, seeds were surface-sterilized by treatment with 70% ethanol for 5 min, followed by commercial bleach (0.5% sodium hypochlorite) containing 0.05% Triton X-100 for 20 min, followed by four washes with sterile distilled water. Seeds were stratified in the dark at 4 °C for 3 d. Then, seeds were sown on half-strength MS medium composed of MS basal salts, 1% agar, and 1% sucrose. The pH was adjusted to 5.7 with potassium hydroxide before autoclaving. Plates were sealed and incubated in a growth chamber at 22 °C under a 16-h light, 8-h dark photoperiod.

Stress-tolerance Tests, Water Loss Measurement and Feeding Experiment

For the drought-tolerance test, plants were initially grown in soil under a normal watering regime for 3 weeks. Watering was then halted and observations were made

after a further 10~12 days without water. When WT plants exhibited lethal effects of dehydration, watering was resumed and the plants were allowed to grow for a subsequent 5 days. For the salt-tolerance test, 3-week-old plants were watered for 12 days at 4-day intervals with increasing concentrations of NaCl of 100, 200, and 300 mM. The survivor was recognized by examining the inflorescence base if it still remains green. For freezing tolerance test, 3-week-old plants (WT and *atgstu17*mutant lines) were grown in a single pot at 22 ^{o}C under 16-h light/ 8-h dark conditions. Three-week-old plants were cold-acclimated (2 ^{o}C) for 12 hours. The samples were transferred into freezer at -6 ^{o}C for 18 hours. After freezing treatment, the plants were grown in normal condition for 10 days and calculated survival rate.

For transpiration (water loss) measurements, detached leaves from 5-week-old plants were exposed to room temperature (25 °C). Leaves were weighed at various time intervals, and the loss of fresh weight (%) was used to indicate water loss.

Exogenous GSH has been used in feeding experiment because it could be taken up by the plant root system (Lappartient & Touraine, 1997; Tausz et al., 2004). For feeding experiment, we germinated the Arabidopsis seeds in Petri dish for 7 days and transferred the seedlings into 1/2 MS agar plate supplemented with GSH or ABA in regular growth condition (22 ^{o}C under 16-h light/ 8-h dark cycles) for two weeks. We analyzed the stability of GSH in the growth medium and found the GSH is stable for 2 weeks (Fig. S2). Or the seedlings were transferred into soil medium in regular growth condition supplemented with GSH or ABA or combinations of GSH and ABA for another 2 weeks. To prevent degradation or oxidation of GSH and ABA, the water solution was replaced every two days with newly prepared chemicals.

Seed Germination and Stomatal Aperture Measurements

Imbibed seeds were cold-treated at 4 ^{o}C in the dark for 3 days, and moved to 22

°C with a 16/8-h light/dark photoperiod. Germination was defined as 1-mm protrusion of the radicle. Epidermal peels were stripped from fully expanded leaves of 5-week-old plants, and were floated in a solution of 30 mM KCl and 10 mM MES-KOH, pH 6.15 in Petri dishes. After incubation for 2.5 h under white light at 22 °C to induce stomatal opening, different concentrations of ABA were added. Stomatal apertures were recorded under an Olympus BX51 system microscope, and were analyzed using DP-PSW software. Measurements were performed using the free software IMAGEJ 1.36b (Broken Symmetry Software; http://brokensymmetry.com).

Histochemical GUS Assay

To investigate *AtGSTU17* gene expression, approximately 1.5 kb of the promoter (-1376 to -1 from the translation initiation codon) was amplified by PCR from genomic DNA. The PCR product was inserted into the pCAMBIA 1391Z vector at the PstI and BamHI sites upstream from the GUS gene. Twenty-five hygromycin-resistant transgenic (T1) plants were obtained. Four single-copy insertion lines were identified by Southern blotting (data not shown). Histochemical assays for GUS activity in transgenic plants were performed as described by Jefferson et al. (1987). Tissues were visualized using an Axiophot microscope (Olympus BX51 system) coupled to a CCD camera.

Subcellular Localization

For subcellular localization, the cDNA fragment containing the *AtGSTU17* coding region without stop codon was amplified by PCR. The PCR product was then inserted downstream from the CaMV 35S promoter and in frame with the 5' terminus of the GFP gene in the pEarlyGate 103 vector (obtained from ABRC) using the Gateway (Invitrogen) system, according to the manufacturer's instructions. The

construct was subsequently delivered into onion epidermal cells by microprojectile bombardment using a PDS-1000/He biolistic particle 18 delivery system (Dupont), essentially according to the manufacturer's instructions. Onion epidermal cell layers were placed on 1% agar plates with half-strength MS salts and bombarded using a rupture disk of 900 Pascal per square inch at a target distance of;10 cm. At 24 h after bombardment, GFP fluorescence was analyzed with the 488-nm argon laser 19 using Olympus BX51 system.

Quantification of the GSH and ABA Content

Leaf tissues of 200 mg were ground with mortar and pestle in the liquid nitrogen. Subsequently, 2 ml of 1 mM EDTA and 6% (v/v) metaphosphoric acid, pH2.8, were added and mixed, then centrifuged at 15000 g for 20 min. Supernatant was neutralized with 0.2 M NaOH. The final pH of the neutralized acid extracts was between 5 and 6. The methods used to measure the total level of glutathione (GSH + GSSG) were as described by Griffith (1980). The oxidized glutathione in the supernatant was reduced to glutathione by glutathione reductass. Glutathione was determined in a kinetic assay in which the reduction of 5,5-dithiobis (2-nitrobenzoic acid) (DTNB) to yellow TNB was spectrophotometrically measured at 412 nm.

For determining endogenous ABA contents in aerial parts, leaf tissues of 200mg harvested at appropriate stages were treated with extraction buffer (80% methanol and 2% glacial acetic acid) for 24 h under darkness, followed by centrifugation for 10 min at 2,000*g*. Supernatants were taken up and dried in a speedvac, then resuspended in 100% methanol plus 0.2 M $NH_4H_2PO_4$ (pH 6.8) for 10 min. To avoid plant pigment and other nonpolar compound effects on the immunoassay, the extracts were first passed through a polyvinylpolypyrrolidone column and then C18 cartridges. Elutes were concentrated to dryness in a speedvac and resuspended in Tris-buffered saline

for immunoassay (Hsu and Kao, 2003). For ABA determination, ABA was quantified by ELISA (Phytodetek ABA kit; Agdia) according to the manufacturer's protocol.

RNA Isolation and Quantitative Real-time (q)RT-PCR Analysis

Total RNA samples were isolated from various plant tissues with the Rezol™ C&T reagent (PROtech, Taiwan). For the RT-PCR, SuperScript III M-MLV Reverse Transcriptase (Invitrogen; http://www.invitrogen.com) was used, following the manufacturer's instructions. The resulting single-stranded cDNA was then used as the template in a qRT-PCR. qRT-PCRs were carried out with gene-specific primers, designed using Vector NTI 9.0 Software. For the qRT-PCR experiments, KAPA SYBR Premix ExTaq was used according to the manufacturer's instructions (KAPA Biosystems, USA) using the BIO-RAD MyiQ™ (Hercules, CA, USA). qRT-PCR experiments were carried out in three separate biological replicates. Primers used for the qRT-PCRs are listed in Table 3.

Microarray Analysis

Three independent biological replicates of microarray experiments were performed using 4-week-old WT and *AtGSTU17*-knockout plants grown under normal conditions. Total RNA was isolated from the rosette leaves using Rezol™ C&T reagent (PROtech, Taiwan). One μg of total RNA was amplified by a Quick-Amp Labeling kit (Agilent Technologies, USA) and labeled with Cy3 or Cy5 (CyDye, PerkinElmer, USA) during the *in vitro* transcription process. CyDye-labled cRNA (0.825 μg) was fragmented to an average size of about 50-100 nucleotides by incubation with fragmentation buffer at 60 ^{o}C for 30 minutes. Correspondingly fragmented labeled cRNA is then pooled and hybridized to Agilent Arabidopsis V4

Oligo 4×44K Microarray (Agilent Technologies, USA) at 60 °C for 17 h. After washing and drying by nitrogen gun blowing, microarrays are scanned with an Agilent microarray scanner (Agilent Technologies, USA) at 535 nm for Cy3. Scanned images are analyzed by Feature extraction 9.5.3 software (Agilent Technologies, USA), and normalization software is used to quantify signal and background intensity for each feature. Genes exhibiting more than a 2-fold enhanced or reduced transcription level in three independent experiments were considered to show significant alterations in expression, and *P* values for the Benjamini and Hochberg method (false discovery rates; FDR) were calculated by by Genespring 11 (Agilent Technologies, USA).

RESULTS

AtGSTU17 Gene in *Arabidopsis thaliana*

In *Arabidopsis thaliana*, the *AtGSTU17* gene consists of two exon and one intron, and locates on the first chromosome. In TAIR database, *AtGSTU17* gene has 1278 bp in total, and the coding sequence has 684 bp. This gene encodes a 227-amino-acid polypeptide (25.3 kD) with an isoelectric point of 6.54 according to sequence prediction. *AtGSTU17* encodes a glutathione S-transferase. It belongs to the Tau class (Fig. S1) GST family.

According to the expression pattern under various conditions by Arabidopsis eFP Browser, *AtGSTU17* can be induced by salt stress, osmotic stress, cold stress and drought stress (Fig. S3). *AtGSTU17* was expressed in stems, leaves, and flowers, but has lower expression levels in root and matured siliques (Fig. S4). *AtGSTU17* can be induced by ABA and expressed in mesophyll and guard cell (Fig. S5 and S6). The expression of *AtGSTU17* also shows a circadian rhythm (Fig. S7).

AtGSTU17 Affects *Arabidopsis* Developments

Two independent T-DNA insertions of *AtGSTU17*, *atgstu17-1* (SALK_139615) and *atgstu17-2* (SALK_025503) are located in the second exon and first intron of *AtGSTU17* (Fig. 1A). RT-PCR analyses indicated that *atgstu17-1* and *atgstu17-2* were null mutants (Fig. 1B). First, We observed a delay flowering phenotype in *atgstu17* mutants (*atgstu17-1* and *atgstu17-2*) under long-day condition(16 h light/8 h dark)(Fig. 2A) and this phenomenon is more significant under short-day condition(12 h light/12 dark)(Fig. 3A). The *atgstu17* mutants exhibited a smooth elliptical leaf shape, and a profusely growing root system (Fig. 3B) and delayed flowering time which produced a leaf number of 27 in contrast to 17 for wild-type (WT, Col-0) plants (Fig. 3C). In contrast, ectopic expression of *AtGSTU17* under the control of the CaMV35S promoter in WT, *GSTU17OE-1* and *GSTU17OE-2*, confirmed by RNA-gel

blotting (Fig. 1C), resulted in an uneven leaf surface and root system similar to WT plants but had an earlier flowering time and only produced a leaf number of 12 (Fig. 3).

Tolerance to Drought and Salt Stresses of the *atgstu17* Mutants

Since *AtGSTU17* was induced by exogenous ABA (Jiang et al., 2010), we investigated the response to prolonged periods of drought and found that both *atgstu17-1* and *atgstu17-2*, had improved resistance to water deficits (Fig. 4A and 4B). Nearly all of the *atgstu17* plants had recovered and begun to grow again, while only 40% of the WT could resume growth. *GSTU17OE* plants did not exhibit a difference in water deficit compared to WT plants (Fig. 4C). Enhanced salt stress tolerance of the *atgstu17-1* and *atgstu17-2* was also observed (Fig. 4D and 4E). However, *GSTU17OE* did not exhibit a difference in salt tolerance compared to WT plants (Fig. 4F). But in freezing treatment, *atgstu17-1* and *atgstu17-2* did not show more tolerance compared to WT plants (Fig. 5)

To confirm that the mutated *AtGSTU17* was the cause of these phenotypes, the *atgstu17-1* and *atgstu17-2* were transformed with a cDNA of *AtGSTU17* driven by the 35S promoter. These 35S:*AtGSTU17*/*atgstu17* transgenic plants showed the leaf morphology, bolting time, and sensitivity to drought stress were similar to WT plants (Fig. 6), verifying the role of AtGSTU17 in plant growth and development.

Effect of Abiotic Stresses on AtGSTU17 Gene Expression.

To assess if *AtGSTU17* can play a role in plant stress responses, a wide spectrum of abiotic stressors was assessed. We observed up-regulation of *AtGSTU17* mRNA levels after practically all employed stimuli (Fig. 7). The most pronounced and persistent induction took place after treatment with the stress hormone ABA, with the

transcript level steadily increased without saturation after 12 h of stimulation. Drought, cold and NaCl treatment resulted in similar transient mRNA elevation that declined within 12 h. The increase in *AtGSTU17* transcript levels occurred as soon as the increase in *RD29A* and *RD22* (marker genes for abiotic stresses) transcripts, or earlier than the marker gene of cold. *AtGSTU17* could also be induced slightly by oxidative stress (paraquat).

Tissue-specific expression of the AtGSTU17 protein

It has been reported that most of the GFP fusions of AtGSTUs, including AtGSTU17 is localized in the cytosol (Dixon et al., 2009). For subcellular localization of the protein, *AtGSTU17* cDNA was fused in frame to the N-terminal side of the GFP marker gene and expressed in transgenic Arabidopsis under the control of the cauliflower mosaic virus (CaMV) 35S promoter (Fig. 8A). Confocal imaging of GFP revealed that the *AtGSTU17*-GFP fusion protein accumulated in the cytosol and nucleus in the onion epidermal cells (Fig. 8B) and in the protoplast of Arabidopsis (Fig. 8C).

In transgenic Arabidopsis expressing the GUS reporter gene driven by the *AtGSTU17* promoter (Fig. 9A), GUS activity was mainly observed in guard cells surrounding hydathodes, trichomes, the shoot and root apical meristems, lateral root primordial, and vascular tissues (Fig. 9, B-D). Strong GUS expression was observed in guard cells and lateral root primordia as well as vascular tissues under ABA treatment (Fig. 9E) and NaCl (Fig. 9F) and mannitol treatments (Fig. 9G).

The *atgstu17* Mutants Exhibit a Reduced Water Loss and Smaller Stomatal Aperture

As a reduction in stomatal pore aperture size mediated by ABA is a critical aspect

of the response of plants to drought stress, we speculated that the enhanced drought resistance of the *atgstu17* plants might be correlated with an altered response to water scarcity. Indeed, the rate of water loss from *atgstu17s* (*atgstu17-1* and *atgstu17-2*) was lower than that from WT plants, as measured by the fresh-weight loss of detached leaves (Fig. 10).

We found that stomata of *atgstu17* had a constitutively reduced aperture (Fig. 11, A and B). ABA treatment reduced the stomatal aperture to a similar extent in mutant and WT plants when the smaller initial aperture of *atgstu17* was taken into account. This constitutively smaller aperture size of stomata may explain the observed lower water loss rate of detached leaves by the *atgstu17* plants (Fig. 10). The stomatal aperture response to ABA treatment in *GSTU17OE* was similar to that of WT plants (data not shown).

The *atgstu17* Mutants Show Altered Physiological Responses Regulated by ABA

Since expression of *AtGSTU17* was induced by ABA , we speculated that germination of mutant seeds in responding to ABA might be altered. At a concentration of 2 μM ABA the germination rate of *atgstu17* was 50% compared to no germination in WT seeds (Fig. 12). In contrast, germination of the *GSTU17OE* seeds was similar to that of WT plants. This indicates that germination of *atgstu17* seeds was less sensitive to ABA.

Root development is also sensitive to ABA (Sharp & LeNoble 2002, De Smet et al. 2006) and this was further studied in *AtGSTU17* mutants. Under white light and unstressed condition for 2 weeks, root lengths among WT, *atgstu17* and *GSTU17OE* plants were similar (Fig. 13A). However, the *atgstu17* mutant was significantly less sensitive to ABA suppression of primary root and lateral root elongation (Fig. 13B), while *GSTU17OE* appeared to be more sensitive compared to WT plants (Fig. 13C).

To more-systematically evaluate the effects of ABA, mutant plants were grown on vertical half-strength MS agar plates supplemented with various concentrations of ABA (0~5 μM). Whereas primary root lengths were reduced by 50% in the presence of 5 μM ABA in 2-week-old *atgstu17* plants, they were reduced by 70% in WT plants (Fig. 13D). The number of lateral roots longer than 0.5 cm per cm of primary root was significantly suppressed in *atgstu17* compared to WT ones under control and ABA treatment conditions (Fig. 13E). The average lateral root length was much greater in the *atgstu17* plant than WT plants in the control and in the presence of ABA (Fig. 13F).

In contrast, primary root lengths of *GSTU17OE* were similar to the WT plants in control condition but were reduced in the presence of 5 μM ABA (Fig. 13, C and G). The lateral root number per cm of primary root of the *GSTU17OE* is significantly greater than the WT plants only in the 5 μM ABA treatments, but the average lateral root length of the *GSTU17OE* did not differ from the WT plants (Fig. 13, H and I).

The *atgstu17* Has Higher GSH and ABA Contents Compared to WT Plant

Using the model xenobiotic substrate CDNB as well as BITC (benzylisothiocyanate) to measure GSH-conjugating activities, AtGSTU17 exhibited high specific activity when compare to other GSTs (Dixon et al., 2009). To investigate whether *AtGSTU17* mutations affected GSH levels during vegetative growth, we measured GSH in leaves and roots of WT and all mutant plants under normal growth conditions. GSH levels in the *atgstu17*s were significantly higher than that in WT plants (Fig. 14A). GSH contents in roots of *atgstu17*s were also greater than that of WT and *GSTU17OE* plants (Fig. 14A). In previous report, the GSH/GSSG ratio was significantly higher in the *atgstu17* than in the WT plants under normal growth conditions (Jiang et al., 2010). Taken together, loss-of-function of *AtGSTU17*

contributed to an increased level of GSH and redox potential in plants growing in normal growth conditions.

Because the stress tolerant phenotype of the *atgstu17*, we suspected that ABA content might be altered in the *AtGSTU17*-mutant plants. Surprisingly, the ABA content in leaves was respectively 2- and 2.3-fold significantly higher in the *atgstu17-1* and *atgstu17-2* than in WT plants, whereas content was lower in the overexpressors than in WT plants (Fig. 14B). ABA-deficient mutant *aba2* (GLUCOSE INSENSITIVE 1 or GIN1), which contains low level of ABA, was used as a reference, and had approximately 1/3 of the WT level of ABA.

Exogenous GSH Induced ABA Accumulation in Planta

We hypothesized that the accumulation of ABA in the *atgstu17* lines was resulted from higher GSH content. To test this hypothesis, WT plants were grown in the solution with or without GSH for two weeks, and the leaf ABA content was measured. The plants grown in solution containing 200 μM GSH accumulated an ABA level that was 1.8-fold greater than the level detected in plants without exogenous GSH treatment (Fig. 15). Plants treated with 400 μM GSH showed 1.4-fold higher ABA content. Our results support that ABA accumulation can be promoted by exogenous GSH treatment.

Effects of Exogenous GSH and ABA on Seed Germination, Stomata Aperture Size, Root architecture and Stress Tolerances

Knowing that GSH and ABA accumulated to higher extents in the *atgstu17*, we investigated the effect of these two chemicals separately and in combination on Arabidopsis. We found that GSH was able to suppress the germination inhibition caused by ABA. When treated with both GSH and ABA, seeds have a higher

germination rate than seeds treated with ABA alone (Fig. 16A). The effect of GSH on the intrinsic stomata aperture size was not known. Figure 16, B and C showed that stomatal apertures were significantly smaller in plants grown in the GSH-containing solutions.

To evaluate the effect of GSH and ABA on the root architecture, WT seedlings were grown on vertical 1/2 MS agar plates supplemented with various concentrations of GSH and/or ABA for 2 weeks. Whereas primary root lengths were reduced by 33% in the presence of 3 μM ABA in 2-week-old WT plants, they were increased by 62% in plants growing in the 25 and 50 μM GSH (Fig. 17, A and B). However, higher GSH concentrations repressed primary root growth. The number of lateral root longer than 0.5 cm per cm of primary root was significantly increased in various concentrations of GSH (Fig. 17, A and C). The combinations of 3 μM ABA and GSHs slightly suppressed the lateral root number (Fig. 17C). The average lateral root length was much greater in WT seedlings receiving 3 μM ABA, and combinations of 3 μM ABA and GSHs (Fig. 17, A and D). GSH treatment alone had no effect on the lateral root length. We concluded that GSH and ABA have different effect on the root growth and development.

atgstu17 Phenotypes were Abolished by GSH Synthesis Inhibitor

To further elucidate the effect of reduced level of GSH in the *atgstu17* on the phenotypes, we grew *atgstu17* mutants on vertical 1/2 MS agar plate containing 3μM BSO. BSO is a highly specific inhibitor of the first enzyme of GSH biosynthesis, and its application results in the depletion of cellular GSH (Vernoux et al., 2000). The GSH level in BSO treated leaves was reduced compared to the mutants without BSO treatment (Fig. 18A). The *atgstu17* seedlings exhibited root development similar to WT plants by 2 weeks after germination on medium containing 3 μM BSO (Fig. 18B

and 18C), specially in lateral root development and (Fig. 18D and 18E). These observations support that root architecture of *atgstu17* to some extent is attributed to the GSH content. Those results support that GSH accumulation is important factor in root development in *atgstu17s*.

Effects of GSH and ABA on Stress Tolerances

We know the concentrations of GSH and ABA in *atgstu17s* contribute to stomatal closed and root development. Therefore, we want to confirm the effects of GSH and ABA on stress tolerances in *atgstu17s*. To assess if exogenous ABA and/or GSH could confer drought tolerances, we grew WT plants in water containing GSH or ABA or combinations of GSH and ABA. We found that plants growing in water containing 400 μM GSH in the presence or absence of ABA recovered and resumed growth from the drought stress test, while no plants could resume growth in water only (Fig. 19B). Exogenous GSH gave better protection than ABA in drought conditions. For salt-tolerance test, all of the WT plants receiving ABA and/or GSH exhibited enhanced salt stress tolerance and much-delayed leaf chlorosis (Fig. 19B). All of the plants growing in water containing 3 μM ABA or a combination of ABA and GSH resumed growth. Three μM ABA gave better protection than GSH in saline conditions.

From the experiment in Figure 19, we learned that increased GSH level confers drought and salt tolerance of WT plants. To test this observation using different approach, we grew the *atgstu17* in water containing 20 and 50 μM BSO for two weeks and found that it exhibited reduced drought tolerance compared to control mutants (Fig. 20A). BSO treatment also reduces the bolting time of the *atgstu17s* (Fig. 20B). This experiment confirms the direct link between the phenotype of the *atgstu17* and accumulation of GSH.

Global Gene Expression in *AtGSTU17*-Knockout Plants Identified by a GeneChip Analysis

Microarray is a powerful tool to analyze the global gene expression. *AsGATU17* can regulate the root development, stomatal closure and abiotic stresses by accumulating GSH and ABA. But the molecular mechanism is unclear. We were interested in determining if the altered gene expression conferred stress tolerance and in assigning a function to AtGSTU17 as a negative regulatory component of the stress response. A microarray analysis was employed for *atgstu17-2* plants using an Agilent Arabidopsis 2 Oligo Microarray (Agilent Technologies, http://www.agilent.com) which covers >21,000 Arabidopsis genes. Total RNA extracted from 3-week-old seedlings of Col-0 and *AtGSTU17* mutants growing under normal growth conditions was used. Three experiments were performed for each line using different labels, Cy3 or Cy5. Each experiment shows consistent expression profiling using Hierarchical Clustering (Fig. 21). As observed, 1320 genes were found to be upregulated > 2-fold, and 888 genes were found to be expressed by < 0.5-fold compared to WT plants. A large number of transcriptome changes being observed, indicated that the *AtGSTU17* gene has an immense influence to the entire genome. Since the potential functions of limited genes in the dataset were studied, we offer selected comments and observations to illustrate important themes.

Expression profiles of genes with known function are presented in Table 1 where only genes the expressions of which had increased by a ratio of > 1.5-fold or reduced by < 0.5-fold in *atgstu17-2* plants compared to WT plants are listed. Among downregulated genes in *atgstu17*, *PIP2;8* (plasma membrane intrinsic protein 2;8, At2g16850, 0.127-fold) and *ATP binding/kinase/protein Ser/Thr kinase* (At1g51830, 0.035-fold) showed great repression in *atgstu17*-mutants. Other genes repressed in *atgstu17* were *protein serine/threonine phosphatase* (At5g26010, 0.46-fold), and

PIP2;7 (At4g35100, 0.46-fold). Most downregulated genes help improve stress tolerance. It was interesting to note that many protein kinases were repressed, as well as many transcription factor genes in various families including MYB, bZIP, WRKY, and especially a large number of Zinc finger genes; these results imply that the AtGSTU17 serves as an upstream signaling component under abiotic stress conditions. The increased expression of *FLC* (At5g10140, 4.34-fold) and repression of the *FT* (At1g65480, 0.30-fold) agree with the a delayed-flowering phenotype.

Among upregulated genes in *atgstu17* mutants, *AtPLC8* (Phosphoinositide-specific phospholipase C family protein, At3g47290, 173-fold), *AtPLC9* (At3g47220, 20-fold) which catalyzes the hydrolysis of phosphatidylinositol 4,5-bisphosphate into the two second messengers, inositol 1,4,5-trisphosphate and diacylglycerol, and *AREB1* (At1g45249, 24-fold), an ABA-induced ABRE-binding bZIP gene, were highly induced. In addition, several other drought stress-tolerant genes were also induced including *XERICO* (At2g04240, 2.31-fold), one of the RING zinc-finger genes, *RAP2.4* (At1g78080, 2.23-fold), an AP2/DREB-type transcription factor gene, *ENH1* (ENHANCER OF SOS3-1, At5g17170, 2.42-fold), a chloroplast-localized protein gene, and *AnnAt1* (ANNEXIN ARABIDOPSIS 1, At1g35720, 4.16-fold), a $Ca2^{+}$-dependent membrane-binding protein annexin gene. *AtMYB88* (At2g02820; 2.54-fold) has the function of generating normal stomatal patterning (Lai, et al., 2005). The expressions of *XERICO*, *RAP2.4*, *ENH1*, and *AtMYB88* were ABA-independent.

Even though we did not observe a freezing-tolerant phenotype, *atgstu17* did exhibit elevated cold-responsive genes; for example, *KIN1* (At5g15960, 4.59-fold), *KIN2/COR6.6* (At5g15970, 5.46-fold) and *COR15b* (At2g42530, 3.93-fold), three late embryogenesis-abundant proteins also induced by ABA.

Expression of Selected Genes from the Microarray Dataset in the *AtGSTU17* Mutant Lines and WT Plants

For further validation of genes that are upregulated or downregulated in the *atgstu17* mutants, we performed a real-time PCR analysis. The total RNAs isolated from the WT and *atgstu17-2* plants under normal growth conditions were used for the real-time PCR analysis (Fig. 22). Also *GSTU17OE* and *atgstu17-1* were included for comparison.

XERICO, *AREB1*, *Bax inhibitor-1*, *AnnAt1*, *COR15b*, and *AtMYB88* of the *atgstu17-1*- and *atgstu17-2*-mutant lines were all upregulated to expression levels similar to those of the array dataset (Fig. 22). These genes maintained similar expression levels as WT in *GSTU17OE-1* and *GSTU17OE-2* plants except for *XERICO*, which had a slightly lower level. The *PI-PLC* gene was difficult to quantify and exhibited great variations in multiples of expression because the gene probably has no expression in WT and *GSTU17OE* lines, and the residual activity influenced the measurement of the knockout mutant lines. The expression levels of four downregulated genes also agreed with the array dataset (Fig. 22). Again these genes in *GSTU17OE* plants maintained similar expression levels as in WT plants except for *ERD5* and *hydrolase* which had higher expressions than WT plants. In conclusion, the global expression of *atgstu17-2* based on the microarray dataset was validated and can be used to interpret the function of AtGSTU17 in Arabidopsis.

AtGSTU17 Regulation of ABA-Downstream and ABA-independent Gene Expressions under Dehydration Conditions

Using an Agilent GeneSpring GX Analysis to screen our microarray dataset, we found that a total of 112 genes were categorized as stress-responsive genes (Table 2). Among them, only 42 genes were activated by ABA treatment to 1.3-fold compared to those without treatment by screening them from the two websites, the Arabidopsis

eFP Browser and AtGenExpress Visualization Tool (Table 2). Thus AtGSTU17 has an immense influence on ABA-independent gene expressions as well as classical ABA signaling.

To clarify this point, we assayed one ABA-independent gene, *XERICO*, altered in *atgstu17* and six ABA-downstream genes, *ABI1*, *AREB1*, *AREB2*, *AtMYC2*, *COR15B*, and *RD29B*, for comparison (Fig. 23). Under control conditions, gene expressions were the same as those seen in the array dataset. After withholding water for 5 days, *XERICO* of *atgstu17-1* and *atgstu17-2* showed greater induction over the WT and overexpressing mutant lines.

ABI1 expressions were the same for the WT and *AtGSTU17*-mutant lines indicating no effect on the master regulator of the ABA response. *AREB1* under normal conditions exhibited high expression in the *atgstu17*-mutant lines, which had no effect on the induction of downstream genes, because *AREB1* activity is regulated by ABA-dependent multi-site phosphorylation of conserved domains (Furihata et al., 2006; Fujii et al., 2007). After withholding water for 5 days, *atgstu17*-mutant lines unexpectedly had lower expression of *AREB1* than the WT, and *RD29B* was also strongly suppressed. *AREB2* of *atgstu17* plants also was repressed compared to WT plants under drought treatment, while *AtMYC2* was similar to the WT, but was lower than the *GSTU17OE* mutant lines. In conclusion, these experiments provide conclusive evidence that AtGSTU17 plays a role as a regulatory component of the ABA-dependent and -independent signaling pathways upstream of many well-studied transcription factors.

AtGSTU17 Induced by ABA-Dependent and -Independent Pathways under Drought Stress Treatment

We hypothesize that *AtGSTU17* gene expression is only ABA-dependent during dehydration treatment. To test this, two ABA-deficient mutants, *aba2* and *nced3*,

which cannot synthesize ABA because of a lack of the short-chain dehydrogenase/ reductase (SDR) (Cheng et al., 2002), and *NCED* (9-cisepoxy- carotenoid dioxygenase) were respectively assayed under the normal growth conditions and under dehydration treatment. Surprisingly, the ABA-deficient mutants had 3-fold higher expression of *AtGSTU17* than the WT under normal growth conditions, but the aba2- and nced3-mutant lines respectively exhibited 80% and 60% expressions of *AtGSTU17* after 5 days of withholding water (Fig. 23). Taken together, this experiment indicates that the expression of *AtGSTU17* is partially induced by ABA-independent drought stress.

DISCUSSION

atgstu17 plants accumulated higher level of GSH in shoot and root

Recent studies have shown that *AtGSTU17* transcripts were induced by far-red light irradiation and regulated by different photoreceptors, especially phyA. Its loss-of-function mutants resulted in a long-hypocotyl phenotype under FR light and delayed flowering under long-day conditions (Jiang et al., 2010). In this study, we extend the function of *AtGSTU17,* the first member of the large GST family in *Arabidopsis thaliana,* by playing a negative role in drought and salt stress tolerance. The basic observation of accumulation of GSH in shoot and root in the *atgstu17* (Fig. 14A) agrees with AtGSTU17 having high activity among GSTs in Arabidopsis when tested with different substrates (Dixon et al., 2009). Without GST mediation GSH can not be utilized as the substrate for the xenobiotic detoxification (Rouhier et al., 2008). As there are no xenobiotics in the system, the turnover of GSH by the GST may be a contributing function but the co-substrate is unknown. The higher GSH content also could be contributed from the increased expression of *GSH2* in the *atgstu17* mutants (Table 1).

AtGSTU17 Plays a Negative Role in Drought and Salt Stress Tolerance

Stress tolerant phenotype of *atgstu17* can be well-explained by the greater GSH and ABA accumulation, and gene expression patterns. According to microarray dataset of *atgstu17* plants (Table 1), among upregulated genes, *AREB1* and several other drought stress-tolerant genes including *XERICO*, *RAP2.4*, *ENH1*, and *AnnAt1* were induced. The expressions of *XERICO, RAP2.4, ENH1,* and *AtMYB88* are ABA-independent according to the Arabidopsis eFP Browser. XERICO overexpression exhibited a marked increase in drought tolerance (Ko et al., 2006). *RAP2.4* was upregulated by drought and salt treatment, and enhanced drought tolerance when overexpressed (Lin et al., 2008). *AnnAt1* induced by ABA and NaCl

treatment when overexpressed were more drought tolerant than WT plants (Konopka-Postupolska et al., 2009). ENH1 functions in detoxification resulting from salt stress by participating in a salt-tolerance pathway (Zhu et al., 2007). In conclusion, ABA-dependent and ABA-independent stress tolerant transcription factors and other genes are activated in *atgstu17* plants leading to drought and salt tolerant phenotype.

When a gene is repressed and can confer stress tolerance, this gene is usually considered to be a negative regulator of a stress response. Just a few example, knockout mutants of *ABI1*, *ABI2*, *Nuclear protein X1* (*NPX1*), and *Altered expression of APX2 8* (*ALX8*) were more stress tolerant than WT plants, and are considered to be negative regulators (Merlot et al., 2001; Kim et al., 2009; Wilson et al., 2009). In this paper, we show that *atgstu17* exhibited altered transcriptome, metabolites, and morphology of the rosette, and enhanced abiotic stress tolerance. Thus AtGSTU17 plays a negative regulator of drought and salt stress response.

The Role of GSH and ABA in Enhancing Drought and Salt Tolerance

An unexpected observation in this study is exogenous GSH treatment associated with the accumulation of ABA in Arabidopsis (Fig. 15). It is surprising that, despite the widely assumed involvement of GSH in abiotic stress signaling in plants, no GSH-mediated drought and salt stress tolerance in plant have been reported in literatures. These facts underline the link between the loss-of-function of *AtGSTU17* gene and all the phenotypes we have found in the *atgstu17* mutants.

GSH is a determinant of the cellular redox balance, and a major cellular antioxidant. In addition, GSH is an important cellular signaling compound influence many fundamental cellular processes (Foyer and Noctor, 2005). Genetic and other evidence shows that GSH concentration is important in many physiological responses (Foyer and Noctor 2009, and the reference therein). Exposure to drought and salt

stress caused increased formation of ROS and thus oxidative stress. The plants GSH and glutaredoxins are implicated in the response to oxidative and are involved in both detoxification of ROS and transmission of the redox signal (Meyer 2008). The GSH pools in *atgstu17* were 35% higher compared to WT plants (Fig. 14A), and the GSH/GSSG ratio in the *atgstu17* was also significantly higher than WT plants (Jiang et al., 2010). The redox potential difference might be the cause of tolerant phenotype of the *atgstu17* under conditions of stress.

When GSH is depleted, plants frequently exhibit decreased sensitivity to oxidative stress (Kushnir et al., 1995; Grant et al., 1996). Several transgenic plants with elevated levels of GSH have been shown to be resistant to oxidative stress (Foyer et al., 1995; Wellburn et al., 1998). In addition, elevated GSH synthesis by increasing γ-glutamylcysteine synthetase (γ-ECS) activity was shown to correlate with Cd resistance in cultured tomato cells (Chen and Goldsborough, 1994) and chilling tolerance (Kocsy et al., 2000, 2001). During the growing stage, an exogenous supply of GSH alone at 400 μM had an obvious effect of enhancing drought tolerance of WT plants. The effect of enhancing salt tolerance was also evident even at 200 μM GSH because chlorosis of leaf tissues was much delayed compared to WT plants without GSH treatment. Furthermore, if WT plants were exposed to a combination of ABA and GSH, the fitness increased dramatically (Fig. 19), much better than the performance produced by each chemical independently against drought and salt stresses.

An activation of ABA accumulation in Arabidopsis by exogenous GSH provides a link between GSH and drought and salt stress tolerance. ABA accumulation was correlated with increased drought tolerance (Thompson et al., 2007), and conferred drought tolerance in mutants like *enhanced drought tolerance1* (a homeodomain-START transcription factor), *poly(ADP-ribose) polymerase* (*PARP*),

npx1, *isopentenyltransferase* (*IPT*), *XERICO* (a RING-H2 gene), and *alx8* (Ko et al., 2006; Vanderauwera et al., 2007; Rivero et al., 2007; Yu et al., 2008; Kim et al., 2009; Wilson et al., 2009). In *atgstu17* plants the higher ABA levels compared to WT plants under non-stressed conditions are consistent with levels of stress tolerance in these mutant plants. Exogenous ABA increased the drought tolerance compared with plant without ABA treatment was demonstrated previously (Huang et al., 2008).

GSH's Effects on the Stomata Aperture Size and Root Patterning

It was interesting to find that the constitutive stomatal aperture was smaller when the WT plants were grown in a solution containing GSH a situation similar to smaller stomatal aperture in *atgstu17* mutants (Fig. B and C). This probably is an effect of ABA because plants growing in the GSH solution exhibited greater ABA content (Fig. 15).

The astonishing root architecture might have been due to higher levels of GSH accumulation in the loss-of-function *atgstu17* plants, which is consistent with high levels of endogenous GSH enhancing cell division in the root meristematic region leading to root elongation (Vernoux et al., 2000), and exogenous GSH on auxin-induced in vitro root formation (Imin et al., 2007). Low concentrations of GSH (< 50 μM) enhanced primary root elongation, but high concentrations suppressed root growth (Fig. 17). Our observation indicates the effect of an exogenous GSH in modulating the root growth pattern of WT plants, and can mimic the phenotype in the *atgstu17* plants. The effect of ABA on the root architecture differed from that of GSH. When applied exogenously in a well-watered condition, ABA acts as a growth inhibitor to suppress primary root growth (Sharp et al., 2004; Bai et al., 2009) while drought stress inhibits lateral root development of soil-grown plants (Xiong et al., 2006). ABA treatment reduced primary root length but encouraged lateral root growth

(Fig. 17). It was apparent that the root systems in the *atgstu17* plants reflected the effects of different combinations of GSH and ABA.

Our findings support a model as summarized in Figure 24 whereby repressed *AtGSTU17* expression is linked to the accumulation of GSH which associates with the accumulation of ABA. The phenotypes of *atgstu17* can be mostly attributed to the combined effects of GSH and ABA, which explain the molecular mechanism of the repression of *AtGSTU17* gene expression in modulating ABA sensitivity of seed germination, stomatal aperture, root architecture, and drought- and salt-stress tolerance. There must be some mechanism that regulates or represses the expression of *AtGSTU17* in stressful conditions. If this did not occur in the Col-0 background, *AtGSTU17* would be a target of natural selection in order for plant to adapt to adverse environments. The link between genotypes and the expressions of specific GST genes was found in wheat which differed in drought tolerance (Galle et al., 2009). Thus in the whole plant, the repression of *AtGSTU17* may play a role of find-tuning GSH homeostasis, redox status and stress-responsive genes in adaptation to changes in environmental signals.

REFERENCE

Bai L, Zhang G, Zhou Y, Zhang Z, Wang W, Du Y, Wu Z, Song C-P (2009) Plasma membrane-associated proline-rich extensin-like receptor kinase 4, a novel regulator of Ca^{2+} signalling, is required for abscisic acid responses in *Arabidopsis thaliana*. Plant J **60:** 314–327.

Chen IC, Huang IC, Liu MJ, Wang ZG, Chung SS, Hsieh HL (2007) Glutathione S-transferase interacting with far-red insensitive 219 is involved in phytochrome A-mediated signaling in *Arabidopsis*. Plant Physiol **143:** 1189-1202

Chen J, Goldsborough PB (1994) Increased activity of γ-glutamylcysteine synthetase in tomato cells selected for cadmium tolerance. Plant Physiol **106**: 233–239.

Cheng WH, Endo A, Zhou L, Penney J, Chen HC, et al. (2002) A unique short-chain dehydrogenase/reductase in *Arabidopsis* glucose signaling and abscisic acid biosynthesis and functions. Plant Cell **14:** 2723–2743.

Cummins L, Cole DJ, Edwards R (1999) A role for glutathione transferases functioning as glutathione peroxidases in resistance to multiple herbicides in black-grass. Plant J **18:** 285-292.

De Smet I, Zhang H, Inze D, Beeckman T (2006) A novel role for abscisic acid emerges from underground. Trends Plant Sci **11**: 434-439.

Deng Z, **Zhang X**, **Tang W**, **Oses-Prieto JA**, **Suzuki N**, **Gendron JM**, **Chen H**, **Guan S**, **Chalkley RJ**, **Peterman TK**, **Burlingame AL**, **Wang Z** (2007) A proteomic study of brassinosteroid response in Arabidopsis. Mol Cell Proteomics. **6**: 2058–2071.

Dixon DP, Hawkins T, Hussey PJ, Edwards R (2009) Enzyme activities and subcellular localization of members of the Arabidopsis glutathione transferase superfamily. J Exp Bot **60:** 1207-1218

Edwards R, Dixon DP (2005) Plant glutathione transferases. Methods Enzymol **401:** 169–18

Edwards R, Dixon DP, Walbot V (2000) Plant glutathione S-transferases: enzymes with multiple functions in sickness and in health. Trends Plant Sci **5:** 193-196

Foyer CH, Noctor G (2005) Redox homeostasis and antioxidant signaling: a metabolic interface between stress perception and physiological responses. *Plant Cell,* **17**, 1866–1875.

Foyer CH, Noctor G (2009) Redox regulation in photosynthetic organisms: signaling, acclimation, and practical implications. Antiox Red Signa **11:** 861-905.

Foyer CH, Souriau N, Perret S, Lelandais M, Kunert K-J, Pruvost C, Jouanin L (1995) Overexpression of glutathione reductase but not glutathione synthetase leads to increases in antioxidant capacity and resistance to photoinhibition in poplar trees. Plant Physiol **109:** 1047–1057.

Furihata T, Maruyama K, Fujita Y, Umezawa T, Yoshida R, et al. (2006) Abscisic acid-dependent multisite phosphorylation regulates the activity of a transcription activator AREB1. Proc Natl Acad Sci USA **103:** 1988–1993.

Fujii H, Verslues PE, Zhu JK (2007) Identification of two protein kinases required for abscisic acid regulation of seed germination, root growth, and gene expression in *Arabidopsis*. Plant Cell **19:** 485–494.

Gallé A, Csiszár J, Secenji M, Guóth A, Cseuz L, Tari I, Györgyey J, Erdei L (2009) Glutathione transferase activity and expression patterns during grain filling in flag leaves of wheat genotypes differing in drought tolerance: response to water deficit. J. Plant Physiol **166:** 1878-1891

Grant CM, MacIver FH, Dawes IW (1996) Glutathione is an essential metabolite required for resistance to oxidative stress in the yeast *Saccharomyces cerevisiae.* Current Genetics **29:** 511–15.

Griffith OW (1980) Determination of glutathione and glutathione disulfide using glutathione reductase and 2-vinylpyridine. Anal Biochem **106**: 207–212.

Hsu YT, Kao CH (2003) Role of abscisic acid in cadmium tolerance of rice (*Oryza sativa* L.) seedlings. Plant Cell Environ **26:** 867–874

Huang D, Wu W, Abrams SR, Cutler AJ (2008) The relationship of drought-related gene expression in *Arabidopsis thaliana* to hormonal and environmental factors. J Exp Bot **59**: 2991–3007.

Imin N, Nizamidin M, Wu T, Rolfe BG (2007) Factors involved in root formation in *Medicago truncatula*. J Exp Bot **58**: 439–451.

Jefferson RA, Kavanagh TA, Bevan MW (1987) GUS fusions: beta-glucuronidase as a sensitive and versatile gene fusion marker in higher plants. EMBO J **6:** 3901-3907

Ji W, Zhu Y, Li Y, Yang L, Zhao X, Cai H, Bai X (2010) Over-expression of a glutathione S-transferase gene, *GsGST*, from wild soybean (*Glycine soja*) enhances drought and salt tolerance in transgenic tobacco. Biotechnol Lett **32:** 1173-1179.

Jiang HW, Liu MJ, Chen IC, Huang CH, Chao LY, Hsieh HL (2010) A glutathione S-transferase regulated by light and hormones participates in the modulation of *Arabidopsis* seedling development. Plant Physiol **154**: 1646-1658.

Kim MJ, Shih R, Schachtman DP (2009) A nuclear fctor regulates abscisic acid responses in Arabidopsis. Plant Physiol **151**: 1433–1445.

Kitamura S, Shikazono N, Tanaka A (2004) *TRANSPARENT TESTA 19* is involved in the accumulation of both anthocyanins and proanthocyaniins in *Arabiopsis*. Plant J **37:** 104-114

Ko JH, Yang SH, Han KH (2006) Upregulation of an Arabidopsis RING-H2 gene, *XERICO*, confers drought tolerance through increased abscisic acid biosynthesis. Plant J **47:** 343–355

Kocsy G, von Ballmoos P, Suter M, Ruegsegger A, Galli U, Szalai G, Galiba G, Brunold C (2000) Inhibition of glutathione synthesis reduces chilling tolerance in maize. Planta **211:** 528–536.

Kocsy G, von Ballmoos P, Ruegsegger A, Szalai G, Galiba G, Brunold C (2001) Increasing the glutathione content in a chilling-sensitive maize genotype using safeners increased protection against chilling-induced injury. Plant Physiol **127:** 1147–1156.

Konopka-Postupolska D, Clark G, Goch G, Debski J, Floras K, Cantero A, Fijolek B, Roux S, Hennig J (2009) The role of Annexin 1 in drought stress in *Arabidopsis*. Plant Physiol **150:** 1394–1410

Kushnir S, Babiychuk E, Kampfaenkel K, Belles-Boix E, Van Montagu M, Inze D (1995) Characterisation of *Arabidopsis thaliana* cDNAs that render yeasts tolerant toward the thiol- oxidising drug diamide. Proc Natl Acad Sci USA **92**: 10580–10584.

Lai B, Nadeau JA, Lucas J, Lee EK, Nakagawa T, et al. (2005) The *Arabidopsis* R2R3 MYB proteins FOUR LIPS and MYB88 restrict divisions late in the stomatal cell lineage. Plant Cell **17**: 2754–2767.

Lappartient AD, Touraine B (1997) Glutathiowe-mediated regulation of ATP sulfurylase activity, SO_4^{2}- uptake, and oxidative stress response in intact canola roots. Plant Physiol 114: 177-183.

Lin RC, Park HJ, Wang HY (2008) Role of *Arabidopsis* RAP2.4 in regulating light and ethylene-mediated developmental processes and drought stress tolerance. Mol Plant **1:** 42 -57

Loggini B, Scartazza A, Brugnoli E, Navari-Izzo F (1999) Antioxidative defense system, pigment composition, and photosynthetic efficiency in two wheat cultivars subjected to drought. Plant Physiol **119:** 1091–1100.

Loyall L, Uchida K, Braun S, Furuya M, Frohnmeyer H (2000) Glutathione and a UV light-induced glutathione S-transferase are involved in signalling to chalcone synthase in cell cultures. Plant J **25:** 237–245.

Marrs KA (1996) The functions and regulation of glutathione *S*-transferases in plants. Annu Rev Plant Physiol Plant Mol Biol **47:** 127-158.

Marrs KA, Walbot V (1997) Expression and RNA splicing of the maize glutathione S-transferase *Bronze2* gene is regulated by cadmium and other stresses. Plant Physiol **113:** 93-102.

Merlot S, Gosti F, Guerrier D, Vavasseur A, Giraudat J (2001) The ABI1and ABI2 protein phosphatases 2C act in a negative feedback regulatory loop of the abscisic acid signalling pathway. Plant J **25:** 295–303.

Meyer JM (2008) The integration of glutathione homeostasis and redox signaling. J. Plant Physiol **165:** 1390-1403.

Moons A (2003) *Osgstu3* and *osgtu4*, encoding tau class glutathione S-transferases, are heavy metal- and hypoxic stress-induced and differentially salt stress-responsive in rice roots. FEBS Letters **553:** 427–432

Rivero RM, Kojima M, Gepstein A, Sakakibara H, Mittler R, Gepstein S, Blumwald E (2007) Delayed leaf senescence induces extreme drought tolerance in a flowering plant. Proc Natl Acad Sci USA **104:** 19631–19636.

Rouhier N, Lemaire SD, Jacquot J (2008) The role of glutathione in photosynthetic organisms: emerging functions for glutaredoxins and glutathionylation. Annu Rev Plant Biol **59**: 143–66.

Roxas VP, Lodhi SA, Garrett DK, Mahan JR, Allen RD (2000) Stress tolerance in transgenic tobacco seedlings that overexpress glutathione S-transferase/ glutathione peroxidase. Plant Cell Physiol **41:** 1229–1234

Sappl PG, Carroll AJ, Clifton R, Lister R, Whelan J, Millar AH, Singh KB (2009)

The *Arabidopsis* glutathione transferase gene family displays complex stress regulation and co-silencing multiple genes results in altered metabolic sensitivity to oxidative stress. Plant J **58:** 53–68.

Sharp RE, LeNoble ME (2002) ABA, ethylene and the control of shoot and root growth under water stress. J Exp Bot 53: 33-37.

Sharp RE, Poroyko V, Hejlek LG, Spollen WG, Springer GK, Bohnert HJ, Nguyen HT (2004) Root growth maintenance during water deficits: physiology to functional genomics. J Exp Bot **55**: 2343–2351.

Sheehan D, Meade G, Foley VM, Dowd CA (2001) Structure, function and evolution of glutathione S-transferases: implications for classification of non-mammalian members of an ancient enzyme superfamily. Biochem J **360***:* 1-16.

Tausz M, Pilch B, Rennenberg H, Grill D, Herschbach C (2004) Root uptake, transport, and metabolism of externally applied glutathione in *Phaseolus vulgaris* seedlings. J. Plant Physiol **161**: 347–349.

Tepperman JM, Zhu T, Chang HS, Wang X, Quail PH (2001) Multiple transcription-factor genes are early targets of phytochrome A signaling. Proc Natl Acad Sci USA **98:** 9437-9442

Thompson AJ, Andrews J, Mulholland BJ, McKee JMT, Hilton HW, Horridge JS, Farquhar GD, Smeeton RC, Smillie IRA, Black CR, Taylor IB (2007) Overproduction of abscisic acid in tomato increases transpiration efficiency and root hydraulic conductivity and influences leaf expansion. Plant Physiol **143:** 1905–1917.

Vanderauwera S, Block MD, Van de Steene N, van de Cotte B, Metzlaff M, Van Breusegem F (2007) Silencing of poly(ADP-ribose) polymerase in plants alters abiotic stress signal transduction. Proc Natl Acad Sci USA **104**: 15150–15155.

Vernoux T, Wilson RC, Seeley KA, Reichheld JP, Muroy S, Brown S, Maughan

SC, Cobbett CS, Van Montagu M, Inzé D, May MJ, Sung ZR (2000) The *ROOT MERISTEMLESS1/CADMIUM SENSITIVE2* gene defines a glutathione-dependent pathway involved in initiation and maintenance of cell division during postembryonic root development. Plant Cell **12:** 97-110.

Wellburn FAM, Creissen GP, Lake JA, Mullineaux PM, Wellburn AR (1998) Tolerance to atmospheric ozone in transgenic tobacco over-expressing glutathione synthetase in plastids. Physiol Plant **104:** 623–629.

Wilson PB, Estavillo GM, Field KJ, Pornsiriwong W, Carroll AJ, Howell KA, Woo NS, Lake JA, Smith SM, Millar AH, von Caemmerer S, Pogson BJ (2009) The nucleotidase/phosphatase SAL1 is a negative regulator of drought tolerance in Arabidopsis. Plant J **58:** 299-317.

Xiong L, Wang R-G, Mao G, Koczan GM (2006) Identification of drought tolerance determinants by genetic analysis of root response to drought stress and abscisic acid. Plant Physiol **142:** 1065–1074.

Yu H, Chen X, Hong Y-Y, Wang Y, Xu P, Ke S-D, Liu H-Y, Zhu J-K, Oliver DJ, Xiang C-B (2008) Activated expression of an Arabidopsis HD-START protein confers drought tolerance with improved root system and reduced stomatal density. Plant Cell **20:** 1134–1151.

Zhu J, Fu X, Koo YD, Zhu JK, Jenney FE Jr, Adams MW, Zhu Y, Shi H, Yun DJ, Hasegawa PM, Bressan RA (2007) An enhancer mutant of *Arabidopsis salt overly sensitive 3* mediates both ion homeostasis and the oxidative stress response. Mol Cell Biol **27:** 5214–5224.

TABLES

Table 1. Selected genes up- or downregulated at least 1.5-fold in *atgstu17* in leaves identified by the GeneChip analysis.

In total, 1320 genes were found to be upregulated > 2-fold, and 888 genes were found to be repressed by < 0.5-fold compared to WT plants.

Agilent probe ID	Gene and Description[a]	Gene code[b]	Fold-Change[c]	P-value[d]
A_84_P856259	PI-PLC;phosphoinositide-specific phospholipase C family protein	At3g47290	173.17	0.00113
A_84_P576436	ABF2 (ABSCISIC ACID RESPONSIVE ELEMENTS-BINDING FACTOR 2)	At1g45249	22.74	0.00113
A_84_P14639	AtPLC9 (phosphoinositide-specific phospholipase C family protein)	At3g47220	19.98	0.00503
A_84_P258350	KIN2/COR6.6 (COLD-RESPONSIVE 6.6)	At5g15970	5.46	0.03633
A_84_P810688	KIN1 (At5g15960,	At5g15960	4.59	0.04729
A_84_P784210	FLC (FLOWERING LOCUS C)	At5g10140	4.34	0.00674
A_84_P22552	Bax inhibitor-1 family / BI-1 family	At5g47130	4.24	0.01850
A_84_P861798	ANNAT1 (ANNEXIN ARABIDOPSIS 1); calcium ion binding / calcium-dependent phospholipid binding	At1g35720	4.16	0.00843
A_84_P10613	Cor15b	At2g42530	3.93	0.04252
A_84_P20589	PIN5 (PIN-FORMED 5); auxin:hydrogen symporter/ transporter	At5G16530	3.5	0.03633
A_84_P721975	MYB88 (myb domain protein 88); DNA binding / transcription factor	At2g02820	2.54	0.01456
A_84_P10941	ATNHX8 (Arabidopsis thaliana Na+/H+ exchanger 8); lithium:hydrogen antiporter/ sodium ion transmembrane transporter/ sodium:hydrogen antiporter	At1G14660	2.49	0.00503
A_84_P818712	ENH1 (ENHANCER OF SOS3-1)	At5g17170	2.42	0.01288
A_84_P14437	XERICO; protein binding / zinc ion binding	At2g04240	2.31	0.04018
A_84_P806724	RAP2.4 (related to AP2 4); DNA binding / transcription factor	At1g78080	2.23	0.04335

A_84_P16329	APX1 (ASCORBATE PEROXIDASE 1); L-ascorbate peroxidase	AT1G07890	2.33	0.00966
A_84_P115992	CIPK1 (CBL-INTERACTING PROTEIN KINASE 1); kinase	AT3G17510	1.99	0.02315
A_84_P859093	DHAR2; glutathione dehydrogenase (ascorbate)	AT1G75270	1.97	0.06533
A_84_P17139	SNRK2-10/SNRK2.10/SRK2B (SNF1-RELATED PROTEIN KINASE 2.10); kinase	AT1G60940	1.82	0.015303
A_84_P12104	GSH2/GSHB (GLUTATHIONE SYNTHETASE 2); glutathione synthase	AT5G27380	1.68	0.00055
A_84_P23264	PIL5 (PHYTOCHROME INTERACTING FACTOR 3-LIKE 5); transcription factor	AT2G20180	0.63	0.00106
A_84_P22559	SAD1(SUPERSENSITIVE TO ABA AND DROUGHT 1)	AT5G48870	0.53	0.03693
A_84_P809263	PIP3 (PLASMA MEMBRANE INTRINSIC PROTEIN 3); water channel	At4g35100	0.48	0.01394
A_84_P13990	protein serine/threonine phosphatase	At5g26010	0.46	0.04335
A_84_P803062	ERD5 (EARLY RESPONSIVE TO DEHYDRATION 5); proline dehydrogenase	At3G30775	0.33	0.00986
A_84_P784337	FT (FLOWERING LOCUS T)	At1g65480	0.3	0.03633
A_84_P17245	PIP2;8/PIP3B (plasma membrane intrinsic protein 2;8); water channel	At2G16850	0.13	0.00232
A_84_P21908	ATP binding / kinase/ protein serine/threonine kinase	At1g51830	0.04	0.00843
A_84_P17744	auxin-responsive GH3 family protein	At5g13380	0.01	0.00503
A_84_P79105	Hydrolase	At1g66860	0.01	0.00986

[a]Description as given by The Institute for Genomic Research database.

[b]AGI, Arabidopsis Genome Initiative.

[c]Genes with fold change (untreated *AtGSTU17*-knockout plants/untreated Col-0 plants). [d]Change *P* value, which measures the probability that the expression levels of each probe set between *AtGSTU17*-knockout plants versus Col-0 plants are the same.

Table 2. Stress-related genes up- or downregulated at least 1.5-fold in *atgstu17* in leaves identified by the GeneChip analysis.

Agilent probe ID	Gene and Description[a]	Gene code[b]	Fold-Change[c]	Induced by ABA[d]
A_84_P751526	disease resistance protein (TIR-NBS class)	AT1G72920	336.00	○
A_84_P750936	disease resistance protein (CC-NBS-LRR class)	AT1G59218	219.25	
A_84_P19944	disease resistance protein (TIR-NBS class)	AT1G72910	177.94	
A_84_P13393	disease resistance protein (TIR-NBS class)	AT1G66090	137.48	○
A_84_P302140	disease resistance family protein [AT4G19515.1]	AT4G19515	123.60	
A_84_P15946	23.5 kDa mitochondrial small heat shock protein (HSP23.5-M)	AT5G51440	99.26	○
A_84_P589554	disease resistance protein (TIR-NBS-LRR class)	AT5G36930	95.51	○
A_84_P800371	disease resistance protein (CC-NBS-LRR class)	AT1G58807	68.62	
A_84_P12746	RPP13 (RECOGNITION OF PERONOSPORA PARASITICA 13); ATP binding	AT3G46530	66.82	
A_84_P22532	disease resistance protein (TIR-NBS-LRR class)	AT5G41740	63.32	
A_84_P15283	thionin, putative	AT1G66100	63.26	○
A_84_P594938	disease resistance protein (TIR-NBS class)	AT5G46490	57.55	
A_84_P23777	disease resistance protein (TIR-NBS-LRR class)	AT1G63880	56.84	
A_84_P20045	disease resistance protein (TIR class)	AT1G57630	49.36	○
A_84_P11136	LIM domain-containing protein / disease resistance protein-related	AT5G17890	45.01	
A_84_P11679	stress-responsive protein	AT2G23680	41.78	○
A_84_P825937	disease resistance protein (TIR-NBS-LRR class)	AT4G16960	32.77	○
A_84_P10430	disease resistance protein (CC-NBS-LRR class)	AT1G61310	28.30	
A_84_P829740	disease resistance protein (TIR-NBS-LRR class)	AT5G46260	26.41	
A_84_P20646	RPP8 (RECOGNITION OF PERONOSPORA PARASITICA 8)	AT5G43470	23.03	

A_84_P10190	CSA1 (CONSTITUTIVE SHADE-AVOIDANCE1); ATP binding / protein binding / transmembrane receptor	AT5G17880	20.93	
A_84_P15319	ECS1	AT1G31580	17.06	
A_84_P13541	disease resistance family protein	AT2G15080	13.47	
A_84_P16863	disease resistance protein (CC-NBS-LRR class)	AT5G43740	13.45	
A_84_P22572	HSP81-1 (HEAT SHOCK PROTEIN 81-1); ATP binding / unfolded protein binding	AT5G52640	11.78	○
A_84_P590035	trypsin inhibitor	AT2G43535	11.25	
A_84_P11793	disease resistance protein RPP1-WsB-like (TIR-NBS-LRR class)	AT3G44630	11.11	
A_84_P23171	AT-HSFA7A (Arabidopsis thaliana heat shock transcription factor A7A); DNA binding / transcription factor	AT3G51910	9.47	○
A_84_P849621	disease resistance protein (CC-NBS-LRR class)	AT1G58602	9.40	
A_84_P766643	disease resistance protein (CC-NBS-LRR class)	AT5G63020	8.51	
A_84_P15440	17.8 kDa class I heat shock protein (HSP17.8-CI)	AT1G07400	7.68	○
A_84_P183744	disease resistance protein (TIR-NBS class)	AT1G69550	7.51	○
A_84_P10439	BIP3; ATP binding	AT1G09080	7.50	○
A_84_P838143	RPP5 (RECOGNITION OF PERONOSPORA PARASITICA 5)	AT4G16950	7.44	
A_84_P19231	ATHSFA2 (Arabidopsis thaliana heat shock transcription factor A2); DNA binding / transcription factor	AT2G26150	7.14	○
A_84_P760741	disease resistance family protein / LRR family protein	AT3G11010	6.92	○
A_84_P836180	disease resistance family protein	AT2G32680	6.31	○
A_84_P19706	transmembrane receptor	AT5G45000	5.43	○
A_84_P812454	ATGSTF6 (EARLY RESPONSIVE TO DEHYDRATION 11); glutathione transferase	AT1G02930	5.23	
A_84_P855121	leucine-rich repeat family protein	AT5G45510	5.23	

A_84_P859300	HSP81-1 (HEAT SHOCK PROTEIN 81-1); ATP binding / unfolded protein binding	AT5G52640	4.65	
A_84_P18999	ATP binding / protein binding / transmembrane receptor	AT1G72840	4.48	
A_84_P23899	17.6 kDa class I small heat shock protein (HSP17.6B-CI)	AT2G29500	4.27	
A_84_P831135	disease resistance protein (TIR-NBS-LRR class)	AT4G12010	4.27	
A_84_P10611	trypsin inhibitor	AT2G43530	4.23	
A_84_P15908	disease resistance protein (TIR-NBS-LRR class)	AT5G40910	4.19	○
A_84_P14320	ATHSP101 (HEAT SHOCK PROTEIN 101); ATP binding / ATPase	AT1G74310	4.03	○
A_84_P10251	ATPP2-A6 (Phloem protein 2-A6); transmembrane receptor	AT5G45080	3.97	○
A_84_P14579	disease resistance family protein	AT3G23110	3.87	○
A_84_P11731	ATMBF1C/MBF1C (MULTIPROTEIN BRIDGING FACTOR 1C); DNA binding / transcription coactivator/ transcription factor	AT3G24500	3.84	○
A_84_P826776	stress-inducible protein	AT4G12400	3.82	○
A_84_P806805	heat shock cognate 70 kDa protein 3 (HSC70-3) (HSP70-3)	AT3G09440	3.76	
A_84_P21539	disease resistance protein (TIR-NBS-LRR class)	AT5G18360	3.76	○
A_84_P18032	17.4 kDa class III heat shock protein (HSP17.4-CIII)	AT1G54050	3.73	
A_84_P13057	THI2.2 (THIONIN 2.2); toxin receptor binding	AT5G36910	3.67	
A_84_P87609	universal stress protein (USP) family protein	AT1G48960	3.64	
A_84_P23046	disease resistance family protein	AT3G05650	3.45	○
A_84_P556555	heat shock cognate 70 kDa protein 2 (HSC70-2) (HSP70-2)	AT5G02490	3.40	
A_84_P10415	MBP2 (MYROSINASE-BINDING PROTEIN 2)	AT1G52030	3.38	
A_84_P20795	disease resistance protein (CC-NBS-LRR class)	AT1G15890	3.16	○
A_84_P18240	similar to HSP18.2 (HEAT SHOCK PROTEIN 18.2)	AT2G19310	3.03	
A_84_P177914	disease resistance protein (CC-NBS-LRR class)	AT1G59124	2.98	
A_84_P305000	defense-related protein	AT2G23960	2.96	

A_84_P811289	HSP81-2 (EARLY-RESPONSIVE TO DEHYDRATION 8); ATP binding	AT5G56030	2.73	
A_84_P21612	disease resistance protein (CC-NBS-LRR class)	AT5G48620	2.64	
A_84_P287150	HSP81-3 (Heat shock protein 81-3); ATP binding	AT5G56010	2.54	
A_84_P750716	ATP binding / protein binding	AT1G58848	2.50	
A_84_P23712	17.6 kDa class I heat shock protein (HSP17.6A-CI)	AT1G59860	2.41	○
A_84_P23491	RRS1 (RESISTANT TO RALSTONIA SOLANACEARUM 1); transcription factor	AT5G45260	2.36	
A_84_P16329	APX1 (ASCORBATE PEROXIDASE 1); L-ascorbate peroxidase	AT1G07890	2.33	
A_84_P830125	BAG6 (ARABIDOPSIS THALIANA BCL-2-ASSOCIATED ATHANOGENE 6); calmodulin binding / protein binding	AT2G46240	2.29	○
A_84_P10998	SGT1A (Suppressor of G2 (Two) 1A); protein binding	AT4G23570	2.27	
A_84_P763160	disease resistance protein (TIR-NBS-LRR class)	AT4G19510	2.15	
A_84_P839521	CW9; ATP binding	AT1G59620	2.14	○
A_84_P162633	ATEGY3	AT1G17870	2.10	○
A_84_P108732	BIP1; ATP binding	AT5G28540	2.05	
A_84_P806024	HSC70-1 (heat shock cognate 70 kDa protein 1); ATP binding	AT5G02500	2.04	
A_84_P792961	APX1 (ASCORBATE PEROXIDASE 1)	AT1G07890	2.01	
A_84_P242433	disease resistance family protein	AT3G25020	1.99	○
A_84_P15197	dehydrin family protein	AT1G54410	1.89	
A_84_P122072	BIP (LUMINAL BINDING PROTEIN); ATP binding	AT5G42020	1.88	
A_84_P753650	disease resistance protein (CC-NBS-LRR class)	AT1G58602	1.86	
A_84_P15339	disease resistance protein (CC-NBS-LRR class)	AT1G63360	1.84	
A_84_P832193	disease resistance protein (TIR-NBS-LRR class)	AT4G19530	1.77	
A_84_P12697	UVH3 (ULTRAVIOLET HYPERSENSITIVE 3); nuclease	AT3G28030	1.70	

A_84_P19202	ATGSTF9 (Arabidopsis thaliana Glutathione S-transferase (class phi) 9); glutathione transferase	AT2G30860	1.61	
A_84_P18775	disease resistance protein (TIR-NBS class)	AT5G48780	1.58	○
A_84_P15928	ATP binding / nucleoside-triphosphatase/ nucleotide binding / protein binding / transmembrane receptor	AT5G46520	0.60	○
A_84_P21536	disease resistance protein (TIR-NBS-LRR class)	AT5G17680	0.59	○
A_84_P17895	MLO10 (MILDEW RESISTANCE LOCUS O 10); calmodulin binding	AT5G65970	0.58	○
A_84_P829422	disease resistance protein (CC-NBS-LRR class)	AT1G61190	0.56	
A_84_P20891	disease resistance protein (TIR-NBS-LRR class)	AT1G72860	0.56	
A_84_P157715	TIR (TOLL/INTERLEUKIN-1 RECEPTOR-LIKE); transmembrane receptor	AT1G72930	0.55	
A_84_P799368	disease resistance protein (TIR-NBS-LRR class)	AT3G44400	0.55	○
A_84_P825746	HSA32 (HEAT-STRESS-ASSOCIATED 32); catalytic	AT4G21320	0.55	
A_84_P819339	ATP binding / nucleoside-triphosphatase/ nucleotide binding / protein binding / transmembrane receptor	AT3G44670	0.50	
A_84_P20454	disease resistance-responsive family protein / dirigent family protein	AT4G23690	0.50	
A_84_P14460	LCR68/PDF2.3 (Low-molecular-weight cysteine-rich 68); protease inhibitor	AT2G02130	0.49	
A_84_P247205	protein kinase family protein	AT5G57670	0.49	○
A_84_P15572	RPP1 (RECOGNITION OF PERONOSPORA PARASITICA 1)	AT3G44480	0.45	
A_84_P22827	RFL1 (RPS5-LIKE 1); ATP binding / protein binding	AT1G12210	0.42	
A_84_P750611	disease resistance protein (CC-NBS-LRR class)	AT1G50180	0.42	○
A_84_P18631	disease resistance family protein / LRR family protein	AT4G13920	0.42	○
A_84_P17823	disease resistance protein (CC-NBS-LRR class)	AT5G47250	0.41	
A_84_P23544	HSP18.2 (HEAT SHOCK PROTEIN 18.2)	AT5G59720	0.40	○

A_84_P21463	disease resistance-responsive family protein	AT4G38700	0.38	○
A_84_P13792	disease resistance protein (TIR-NBS-LRR class)	AT4G09430	0.35	
A_84_P17039	disease resistance protein (CC-NBS-LRR class)	AT1G61180	0.34	
A_84_P168393	mob1/phocein family protein [AT4G19050.1]	AT4G19050	0.28	
A_84_P233429	disease resistance protein (CC-NBS-LRR class)	AT1G58390	0.24	
A_84_P15125	disease resistance protein (CC-NBS-LRR class)	AT1G51480	0.14	○

[a]Description as given by The Institute for Genomic Research database.

[b]AGI, Arabidopsis Genome Initiative.

[c]Genes with fold change (untreated *AtGSTU17*-knockout plants/untreated Col-0 plants). [d]A hollow circle means the gene activated by ABA treatment to 1.3-fold compared to those without treatment from the two websites, the Arabidopsis eFP Browser and AtGenExpress Visualization Tool

Table 3. Primers used in the qRT-PCR experiments.

Gene	Gene code	Forward primer	Reverse primer
ABI1	At4g26080	GTCGAGATCCATTGGCGATAGA	TGCCATCTCACACGCTTCTTC
Act8	At1g49240	GAGGATAGCATGTGGAAGTGAGAA	AGTGGTCGTACAACCGGTATTGT
AnnAt1	At1g35720	TGATTCTGTTCCTGCTCCTTCTG	TCGTGGTATGCTTGCCTGATG
AREB1/ABF2	At1g45249	GGTGGAGGTGGAGGGTTGACTA	CCATGGCTTGTGTTTCTTCAGC
AREB2/ABF4	At3g19290	AACAACTTAGGAGGTGGTGGTC	CTTCAGGAGTTCATCCATGTTC
AtMYB88	At2g02820	ATCTCTAGCAGCAGGCATCC	GCAAGGAGGTGGTTGTGAAG
AtMYC2	At1g32640	TCATACGACGGTTGCCAGAA	AGCAACGTTTACAAGCTTTGATTG
ATP binging protein	At1g51830	CCCGATTGAAGGTGAAACTC	TGATGATCTCTAACAATACGACTC
Bax inhibitor 1	At5g47130	TTCTCGGCAGTGGCAATG	CCACGAAGAGCAGGAGTC
CAT1	At1g20630	CGCCATGCCGAAAAATACC	TCTTGCCTGTCTGAATCCCA
Cor15b	At2g42530	GCCAATGAAACTGCGACTGAG	GGACTTTGTGGCATTCTTAGCC
ERD5	At3g30775	GCATTGTCCTTCGGGTTAAAGAG	CATCCTCATGAGTTGACGGTCAT
Gstu17	At1g10370	ATGCGTTTCTGGAGAAGGCG	AGCTTTGCAGTCTCGGGCAT
Hydrolase	At1g66860	CAGAGGAAGGCTATGAACATAATG	TTGAGGAGTTAGATTGAGGTCAC
NCED3	At3g14440	CAACGGAGCTAACCCACTTCA	ACCCTATCACGACGACTTCATCT
PIP2;8	At2g16850	GGAGTTGGACTCGTTAAGGCCT	TCAGTGGCGGAGAAGACAGTGTA
PI-PLC	At3g47290	CGATCGGTGACCAGGTTCATC	ACCCTCACACCCTGTTCAAGTG
RD22	At5g52610	AGGTGGCTAAGAAGAACGCACC	TGGCAGTAGAACACCGCGAAT
RD29A	At5g52310	TGCACCAGGCGTAACAGGTAA	TTGTCCGATGTAAACGTCGTCC
RD29B	At5g52300	GCGCACCAGTGTATGAATCCTC	TGTGGTCAGAAGACACGACAGG
XERICO	At2g04240	TCAAGTCTTCCTGGTCCATCAGA	GAAGAAGGCGAGGATGAAGACG
GSH2	At5g27380	GCTAGGCTGCTTATTGAGGAGTC	GAGGCTTCATAACAAACAATCCG

DHAR2	At1g75270	CGAGAAGGCTTTGGTTGATGAG	CGACTCCCTAGAGAACAAAGCCT
SAD1	At5g48870	ATGGCGAACAATCCTTCACAG	CAGAATGGCGATGTTGTTGC

FIGURES

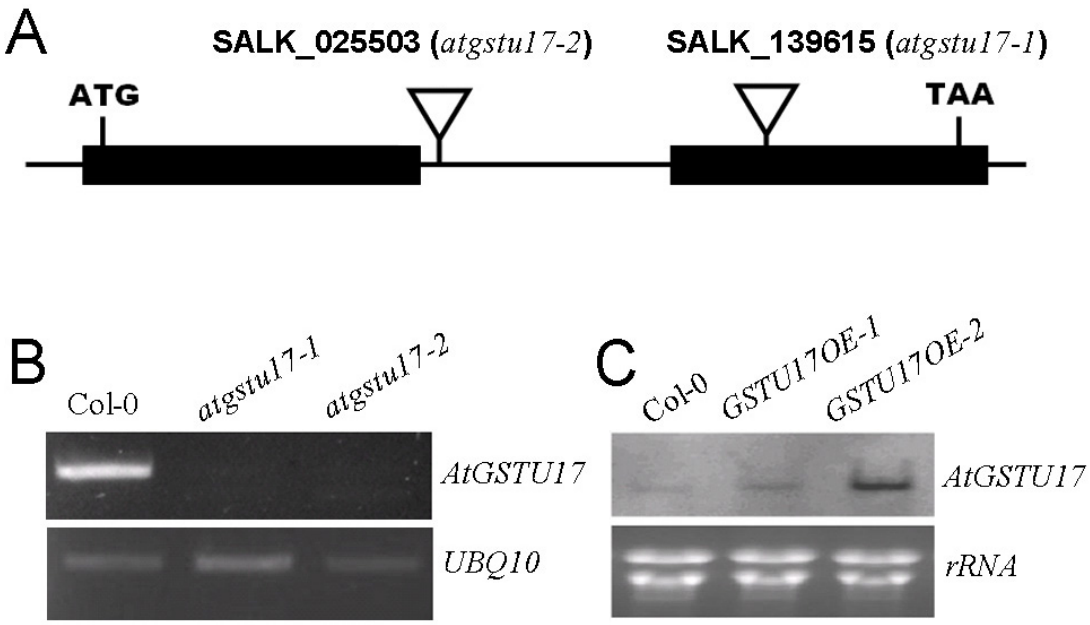

Figure 1. Location of T-DNA insertions in the *AtGSTU17* gene and analysis of *AtGSTU17* knockout and overexpressed transgenic lines.

(A) *AtGSTU17* gene structure and insertional mutation sites of SALK_139615 (*atgstu17-1*) and SALK_025503 (*atgstu17-2*). Square boxes represent exons, and black bars represent introns. T-DNA insertions in the two mutant lines are shown as triangles.

(B) *AtGSTU17* transcripts in Col-0 and two *AtGSTU17* knockout mutants identified by RT-PCR analysis. The expression levels of *AtGSTU17* using specific primers (GST30-L: caaagaagatctttcctaagccgc, GST30-R: caccaaacctgatacatacgtaac) were compared with the *UBQ10* expression (UBQ10-L: gatctttgccggaaacaattggaggatggt, UQB10-R: cgacttgtcattagaaagaaagagataacagg).

(C) RNA-blot analysis of *AtGSTU17* in Col-0 and two transgenic lines overexpressing *AtGSTU17*. 10 μg of total RNA was loaded in each lane. cDNA probes used were DIG-labeled Arabidopsis *AtGSTU17* and rRNA were used as a loading control.

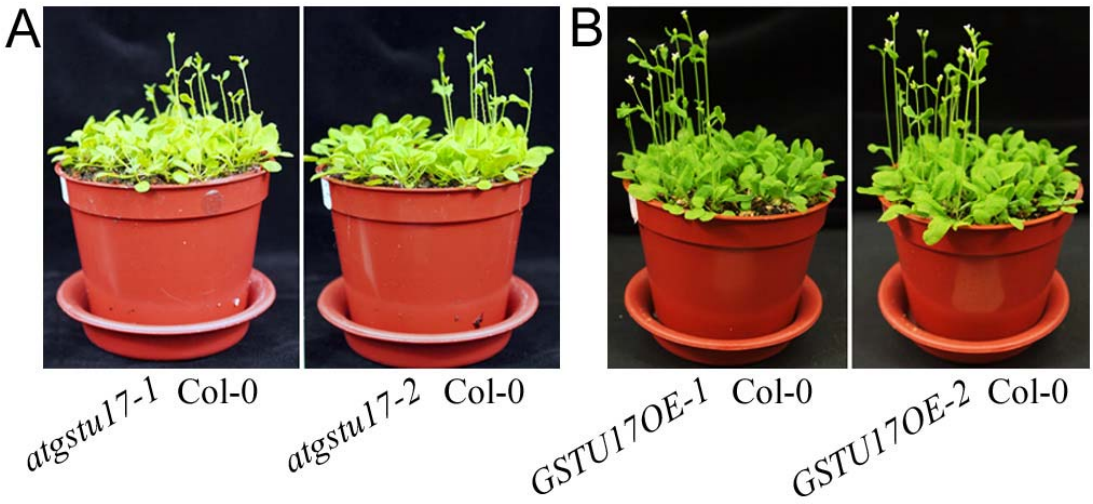

Figure 2. Flowering time of *AtGSTU17*-mutant lines.

(A) 28-day-old plants growing under 16-h light/8-h dark conditions of the Col-0, two knockout mutants, *atgstu17-1* and *atgstu17-2*.

(B) 24-day-old plants growing under 16-h light/8-h dark conditions of the Col-0, two overexpressing lines, *GSTU17OE-1* and *GSTU17OE-2*.

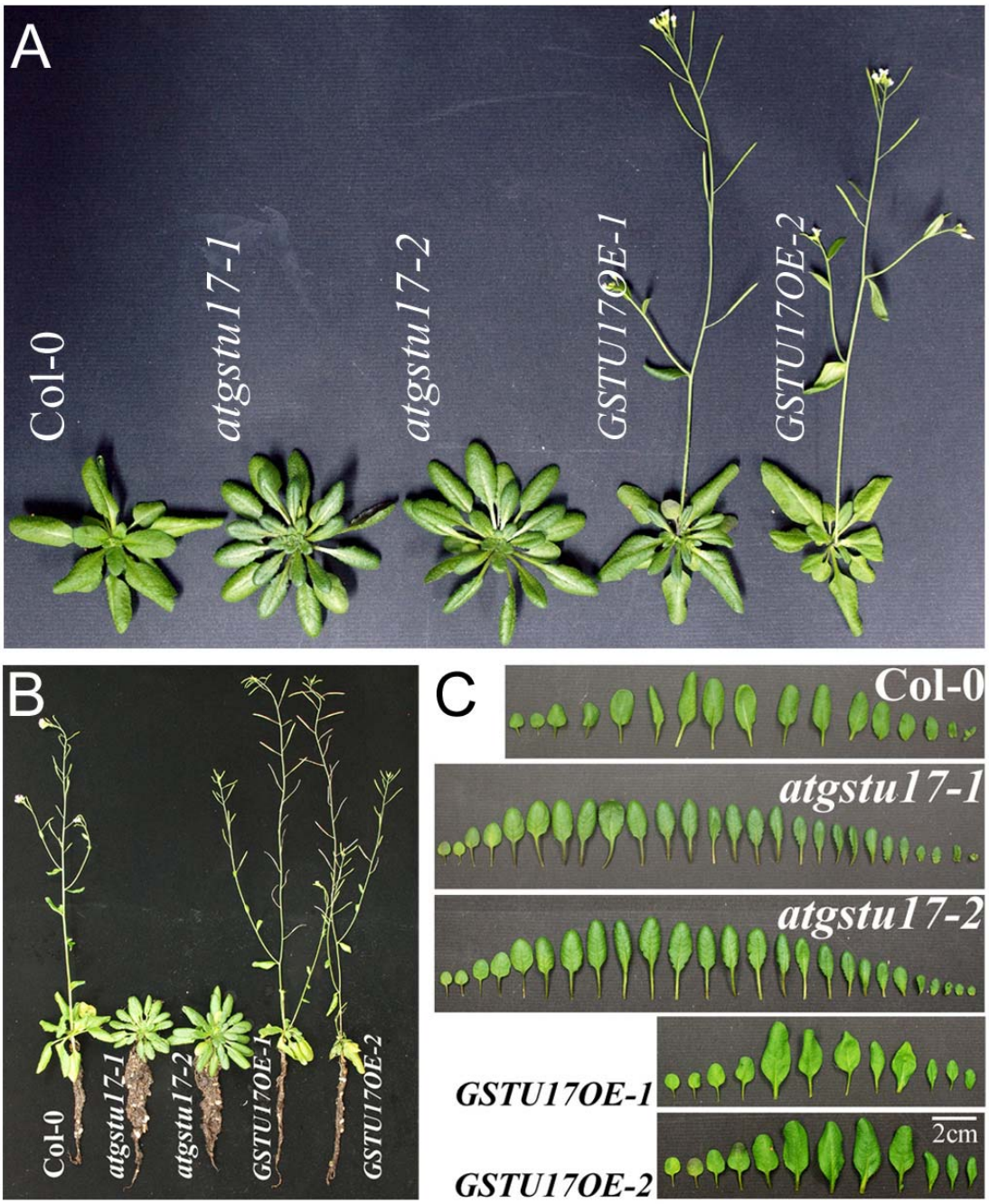

Figure 3. Phenotypes of *AtGSTU17*-mutant lines.

(A) Six-week-old plants growing under 12-h light/12-h dark conditions of the Col-0, two knockout mutants, *atgstu17-1* and *atgstu17-2*, and two overexpressing lines, *GSTU17OE-1* and *GSTU17OE-2*.

(B) Eight-week-old plants. Growth condition is same as A.

(C) Leaf sizes and numbers beginning from the oldest one on the right hand side for different lines of 6-week-old plants under 12-h light/12-h dark.

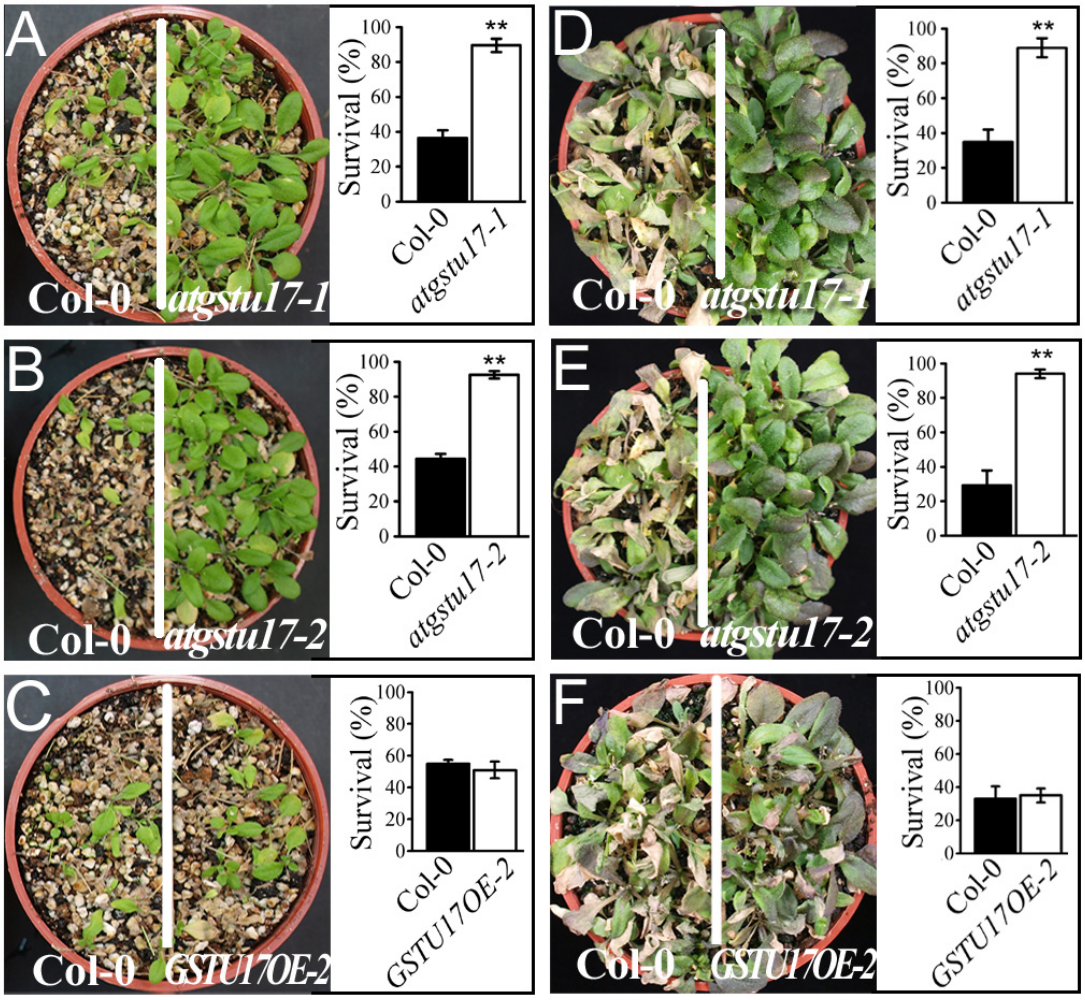

Figure 4. Tolerance to drought and salt stresses of *AtGSTU17*-mutant lines.

(A) and (B) Plants (Col-0, *atgstu17-1* and *atgstu17-2*) were grown in a single pot under 16-h light/ 8-h dark conditions. Watering of 3-week-old plants was withdrawn for 10~12 days and then resumed watering. The photograph and figure showing the differences in the reactions of plants to the short-term drought were taken after 5 days of re-watering.

(C) Same as A but for Col-0 and *GSTU17OE-2*.

(D) and (E) Three-week-old plants (Col-0, *atgstu17-1* and *atgstu17-2*) were watered for 12 days at 4-day intervals with increasing concentrations of NaCl of 100, 200, and 300 mM. The photograph and figure were taken 18 days after the salt treatments. Only the plant having the inflorescence base remaining green

was considered as survivor.

(F) Same as D but for Col-0 and *GSTU17OE-2*.

The survival rates (%) were calculated from the numbers of surviving plants per total plants tested. Data are presented as the means ±standard deviation (SD). Five independent experiments were performed with similar results.

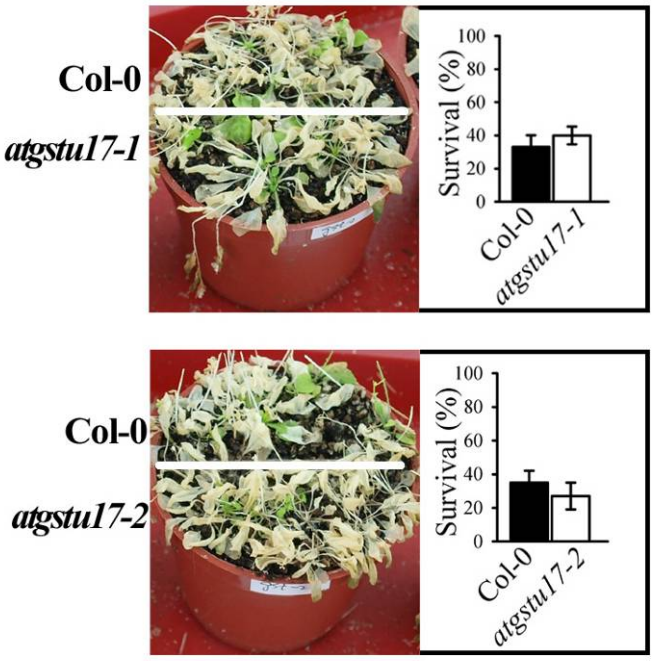

Figure 5. Tolerance to Freezing of *AtGSTU17*-mutant lines.

Plants (Col-0, *atgstu17-1 and atgstu17-2*) were grown in a single pot at 22 ^{o}C under 16-h light/ 8-h dark conditions. Three-week-old plants were cold-acclimated (2 ^{o}C) for 12 hours. The samples were transferred into freezer at -6 ^{o}C for 18 hours. After freezing treatment, the plants were grown in normal condition for 10 days and calculated survival rate. The survival rates (%) were calculated from the numbers of surviving plants per total plants tested. Data are presented as the means ±standard deviation (SD). Three independent experiments were performed with similar results.

Figure 6. Complementation experiment of AtGSTU17 in *atgstu17-1* and *atgstu17-2* plants.

(A) Delayed flowering time in *atgstu17-1* and *atgstu17-2* were rescued in *35S:GSTU17OE-5/atgstu17-1* and *35S:GSTU17OE-3/atgstu17-2* transgenic plants. Photographs were taken of 25-day plants growing in a growth chamber at 22 ^{o}C under a 16-h light, 8-h dark photoperiod.

(B) Drought tolerant phenotype in *atgstu17-1* and *atgstu17-2* were lost in *35S:GSTU17OE-5/atgstu17-1* and *35S:GSTU17OE-3/atgstu17-2* transgenic

plants. Plants were initially grown on soil under a normal watering regime for 3 weeks. Watering was then halted for 10 d and the photographs were taken.

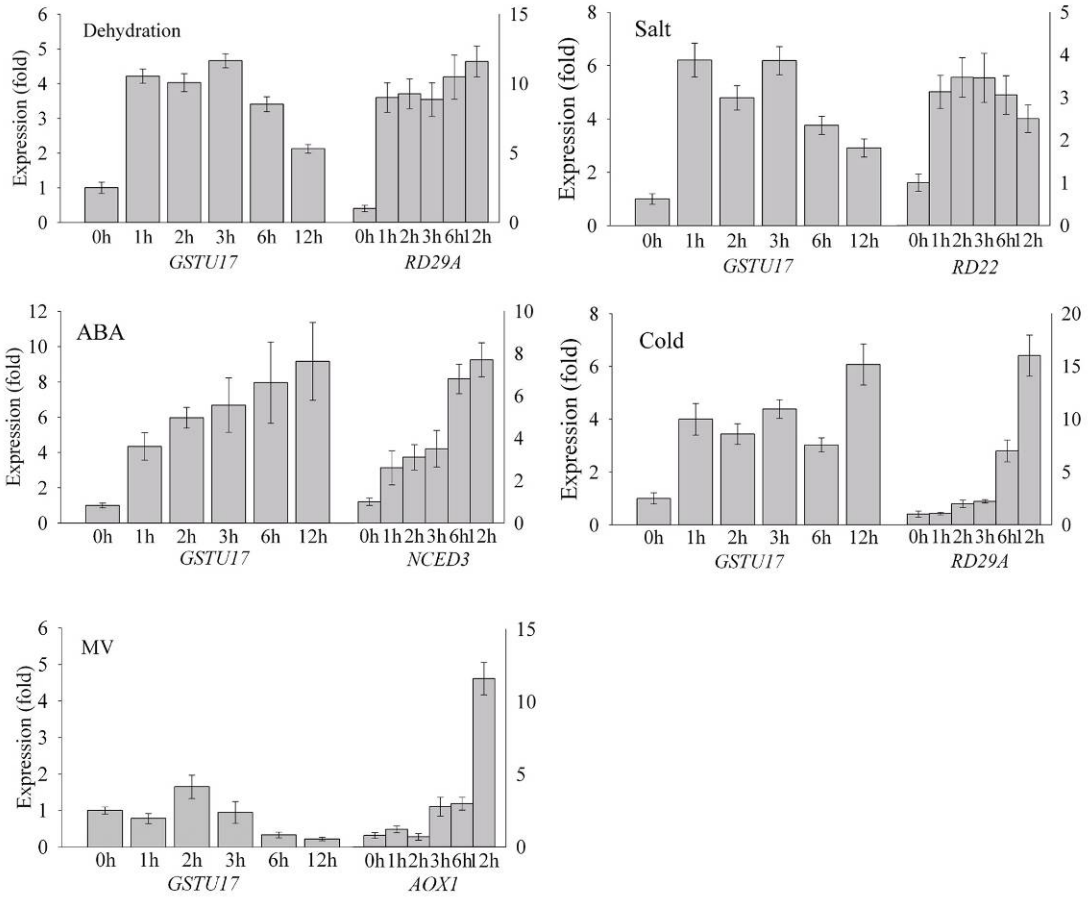

Figure 7. Effects of abiotic stresses and ABA treatments on *AtGSTU17* gene expression.

Quantitative RT-PCRs representing the relative mRNA accumulation of *AtGSTU17* were normalized to those of different known stress-inducible genes. The amplification of *Actin8* was used as an internal control to normalize all data. The level of each gene transcript in wild-type before stress or ABA treatments was set to 1.0. Three independent experiments were performed with similar results. Marker genes were *RD29A* for dehydration and cold, *RD22* for salt, *NCED3* for ABA, and *AOX1* for oxidative stress.

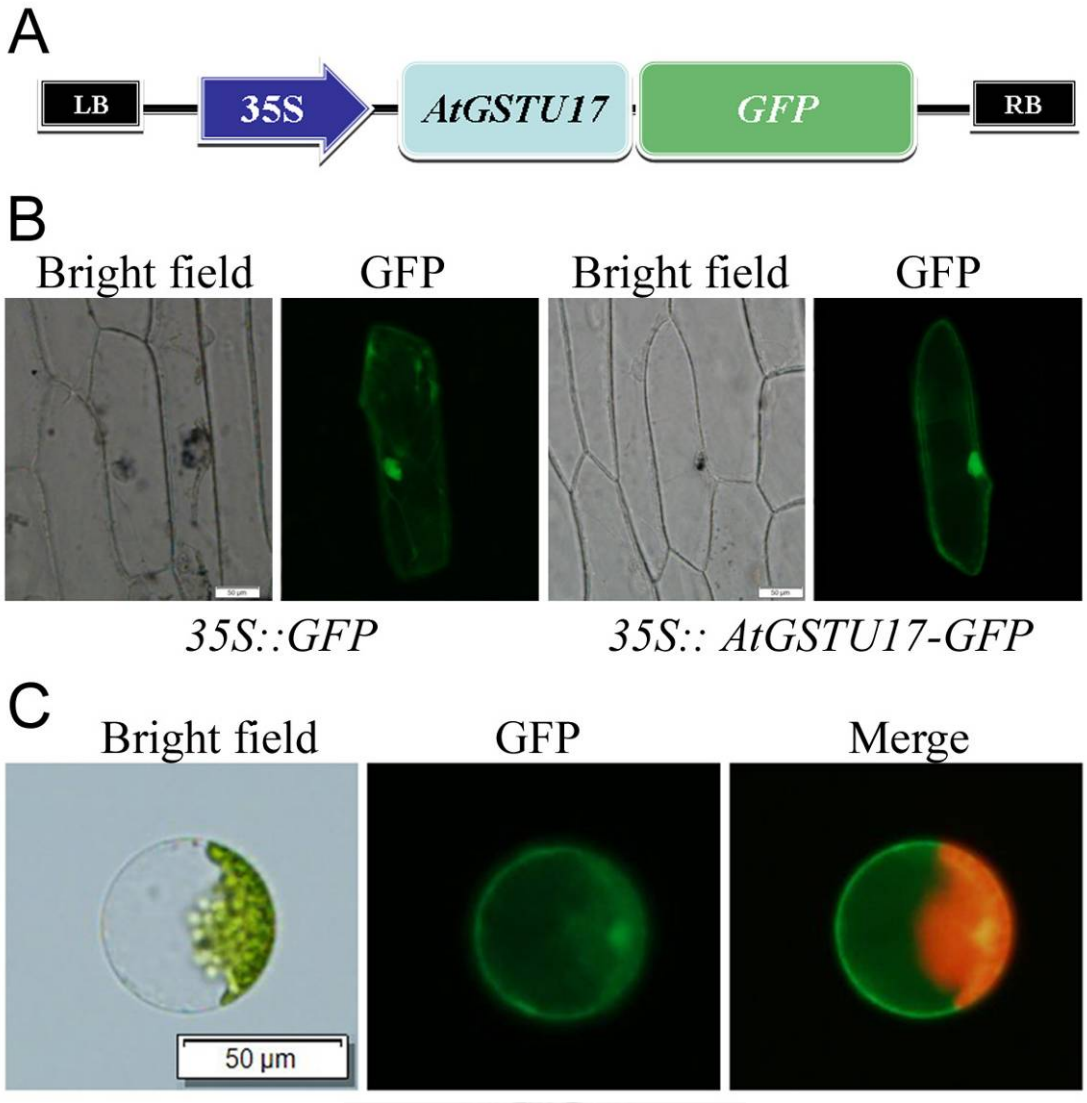

Figure 8. Subcellular localization of AtGSTU17 protein.

(A) Vector construction of *AtGSTU17-GFP* in pEarlyGate 103.

(B) Confocal images of onion epidermal cells. Constructs of *35S:GFP* or *35S: AtGSTU17-GFP* were translocated into onion epidermal cells by particle bombardment.

(C) *35S:AtGSTU17-GFP* fusion were transiently expressed in *Arabidopsis* protoplasts and visualized by bright-field and fluorescence microscopy. The expression of the introduced genes was detected after 16 hours. Scale bars represent 50 μm.

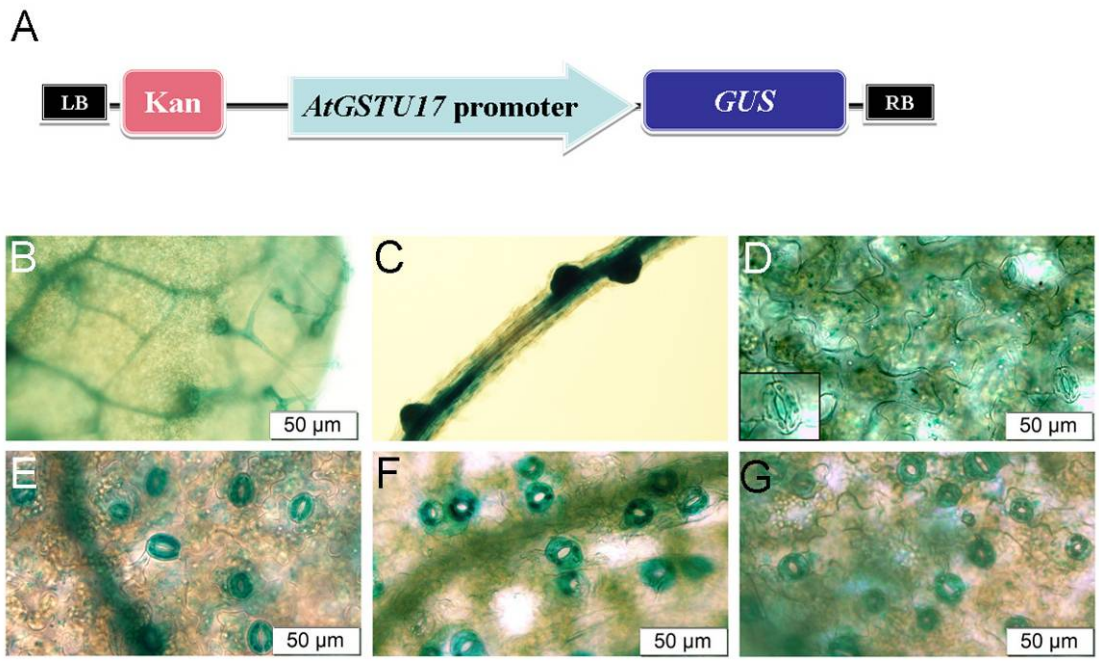

Figure 9. Tissue-specific expression of the AtGSTU17 protein.

(A) The construction of *AtGSTU17* promoter fused GUS gene in pCAMBIA 1391Z vector.

(B) Patterns of *AtGSTU17* promoter-driven GUS expression in vascular cells and trichomes in normal growth condition.

(C) GUS expression in the root in normal growth condition.

(D) GUS expression in the leaf with an insert to show the enlarged stomata in normal growth condition

(E) GUS expression in a leaf treated with 5 μM ABA for 6 h.

(F) GUS expression in a leaf treated with 200 mM mannitol for 6h.

(G) GUS expression in a leaf treated 300 mM NaCl for 6 h.

Two-week-old plants grown on MS agar plates were used for the treatments.

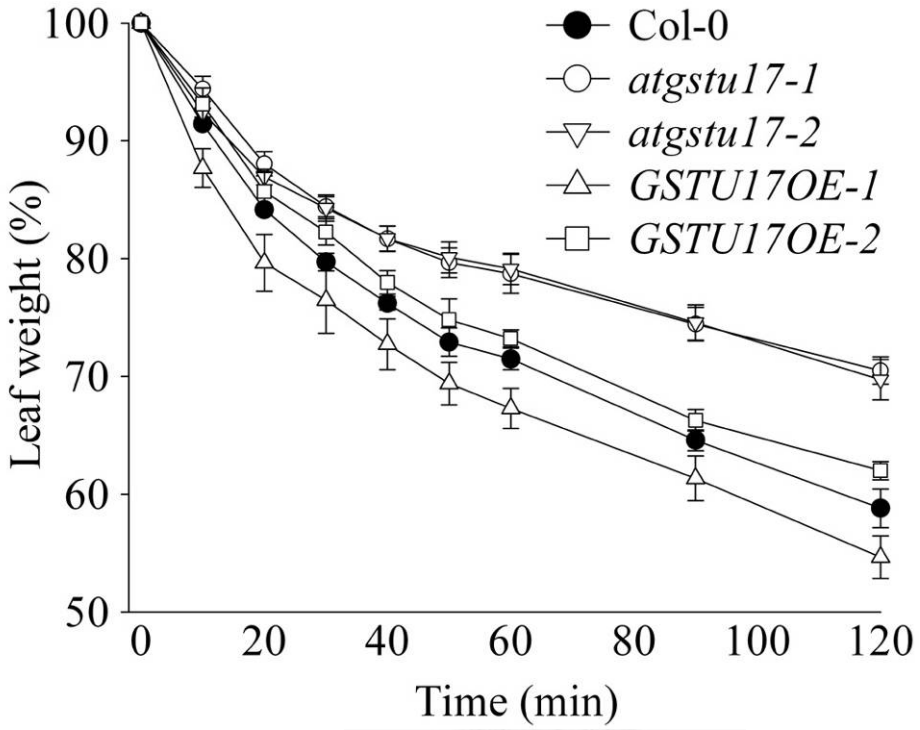

Figure 10. *AtGSTU17* mutation on water loss rates and ABA-mediated stomatal closure.

Progressive water loss from detached leaves as a function of time in 3-week-old Col-0 and *AtGSTU17*-mutant plants. Detached leaves were placed on weighing dishes, and allowed to slowly dry on a laboratory bench (25^{o}C, 60% relative humidity). Weights of the samples were recorded at regular intervals. Error bars represent the standard deviation (SD). Data are presented as the means of water loss percentage ± SD. Three independent experiments were performed with the same trends.

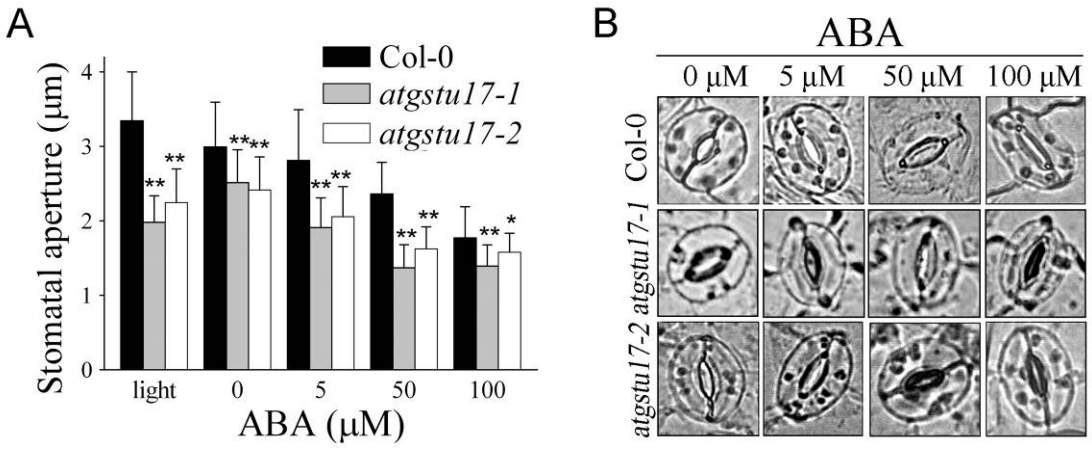

Figure 11. *AtGSTU17* mutation on water loss rates and ABA-mediated stomatal closure.

(A) Effect of the *AtGSTU17* mutation on ABA inhibition of light-induced stomatal opening. Stomata were pre-opened under light for 2.5 h, and then incubated in the indicated concentrations of ABA for 2.5 h under light. Stomatal apertures were measured on epidermal peels. Values are the means and SD (n > 60). *Significantly differs from the Col-0 (p < 0.05), by Student's t-test. These blind experiments were repeated at least three times.

(B) Micrographs representing the dynamics of ABA-mediated stomatal closure in Col-0 and *AtGSTU17*-mutant plants.

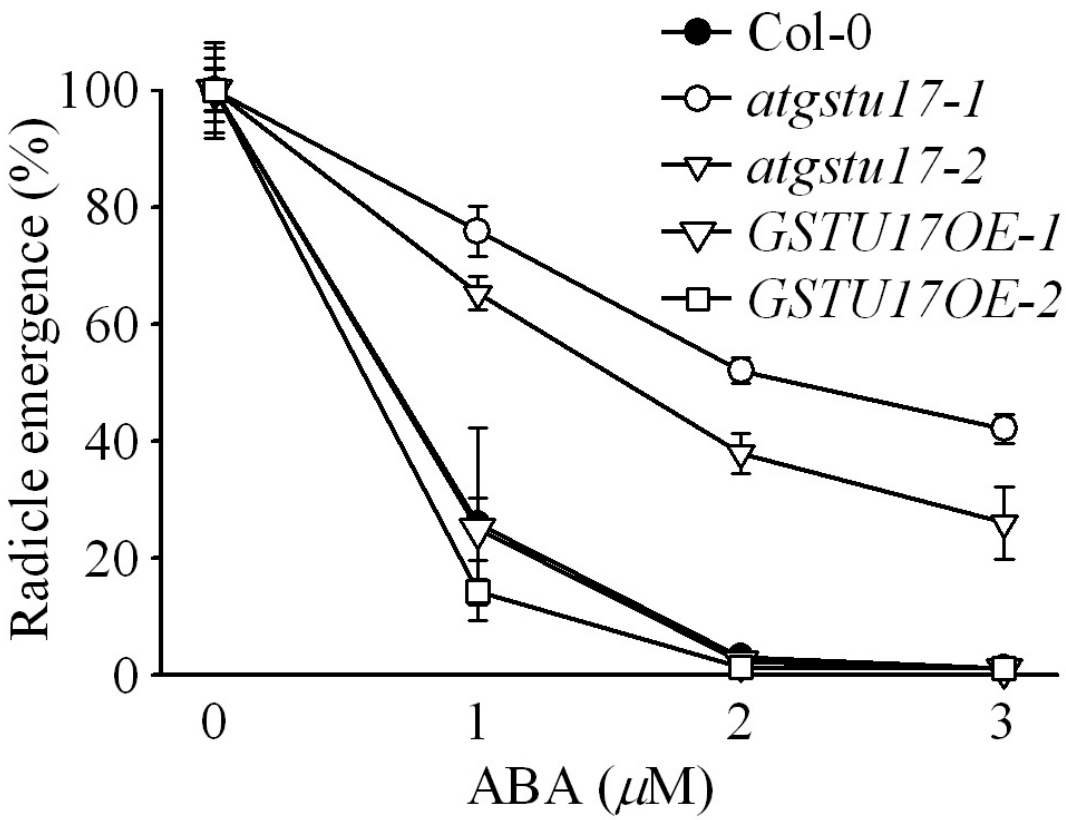

Figure 12. AtGSTU17 regulates seed germination in response to ABA.

Germination percentage of Col-0 and *AtGSTU17*-mutant lines. Data are presented as the means ±standard deviation (SD). Three independent experiments were performed with the same trend. Seedlings were germinated and grown on half-strength MS agar plates with or without ABA for 3 days.

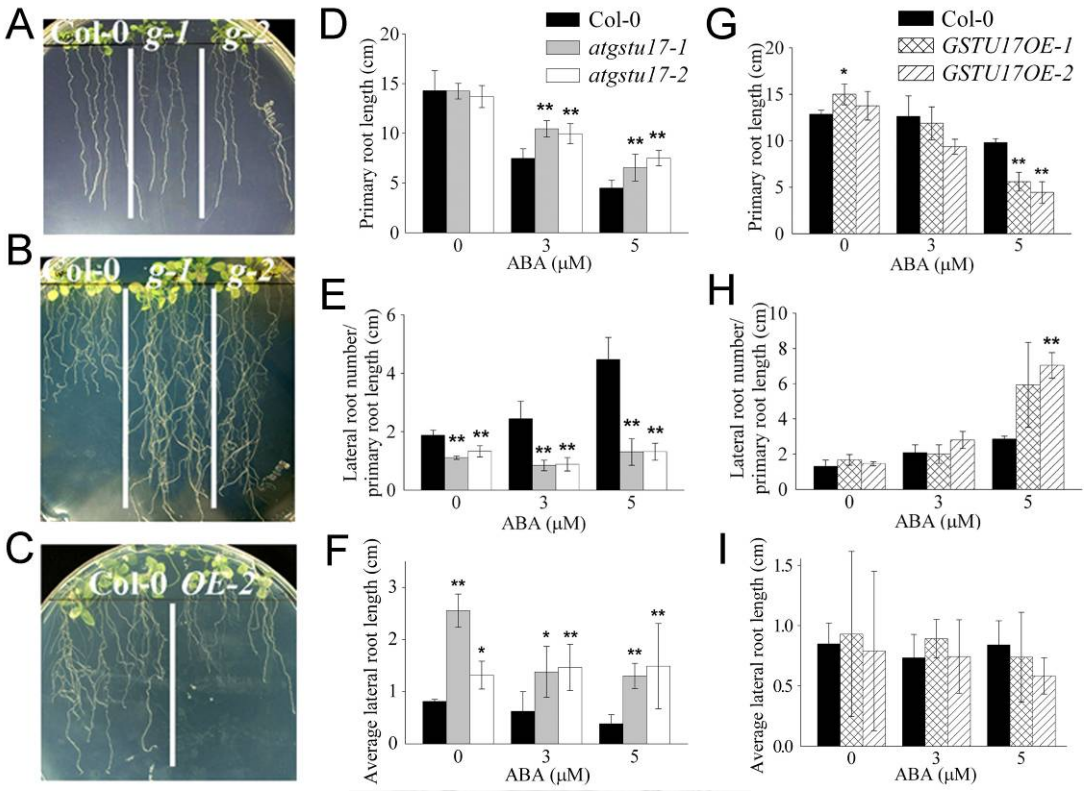

Figure 13. AtGSTU17 regulates lateral root growth in response to ABA.

(A) Seedlings were germinated and grown on 1/2 MS agar plates without ABA for 3 days and were transferred to the same MS medium without ABA for 1 week.

(B) Same as A but the medium supplemented with 3 μM ABA for 2 weeks.

(C) Same as A but the medium supplemented with 5 μM ABA for 3 weeks.

(D) and (G) Comparison of the primary root length.

(E) and (H) Lateral root number per cm of primary root. Only lateral roots longer than 0.5 cm were used for the calculation.

(F) and (I) Average lateral root length.

atgstu17-mutant (D, E and F), *GSTU17OE* (G,H and I) and Col-0 plants grown on vertical 1/2 MS agar plates supplemented with ABA concentrations as indicated for 2 (D, E and F) or 3 weeks (G, H and I). Thirty plants at each ABA concentration were counted and averaged for (D and G). Ten plants at each ABA concentration

were counted and averaged for (E, F, H and I). Three independent experiments were performed with the same trends. Error bars represent the standard deviation (SD) (*t* test; *, $p < 0.05$; **, $p < 0.01$).

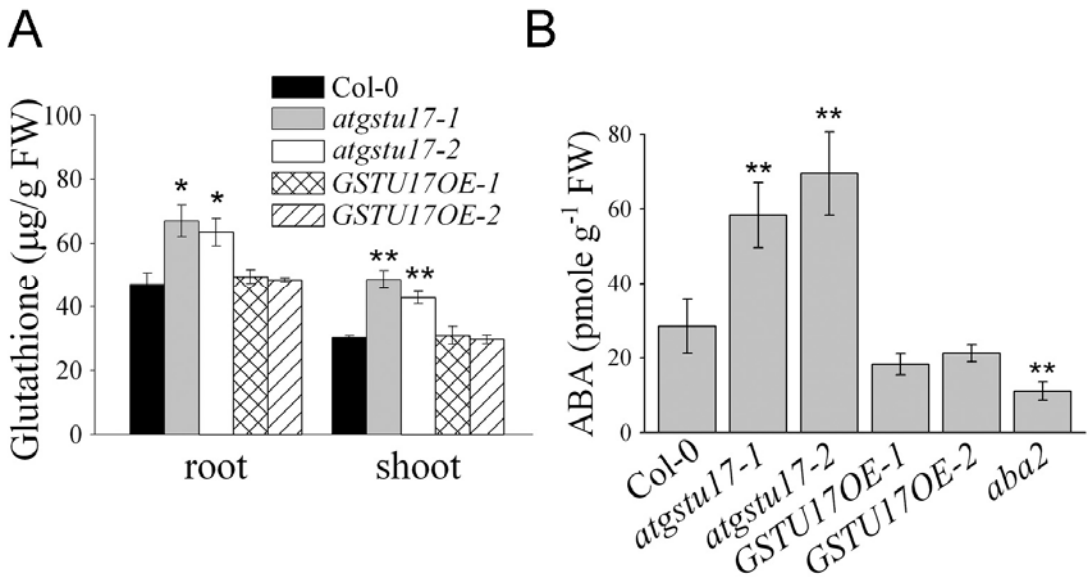

Figure 14. ABA and GSH contents in Col-0 and *AtGSTU17*-mutant plants.

(A) Determination of GSH levels in shoot and root under non-stressed conditions in Col-0 and *AtGSTU17*-mutant plants. Values are presented as the mean ± SD from five samples for each time point. Two independent experiments were performed with similar results. Plants of 3-week-old grown in a growth chamber of 22 ^{o}C under 16-h light/ 8-h dark conditions were used in this study. Three independent experiments were performed with the same trends. Error bars represent the standard deviation (SD) (*t* test; *, $p < 0.05$; **, $p < 0.01$).

(B) Determination of ABA levels under non-stressed conditions in 3-week-old Col-0 and *AtGSTU17*-mutant plants. Plants were grown in a growth chamber of 22 ^{o}C under 16-h light/ 8-h dark conditions. Values represent the means ± standard deviation (SD) from three independent sets of samples. Three independent experiments were performed with similar results. *aba2* was used as a reference.

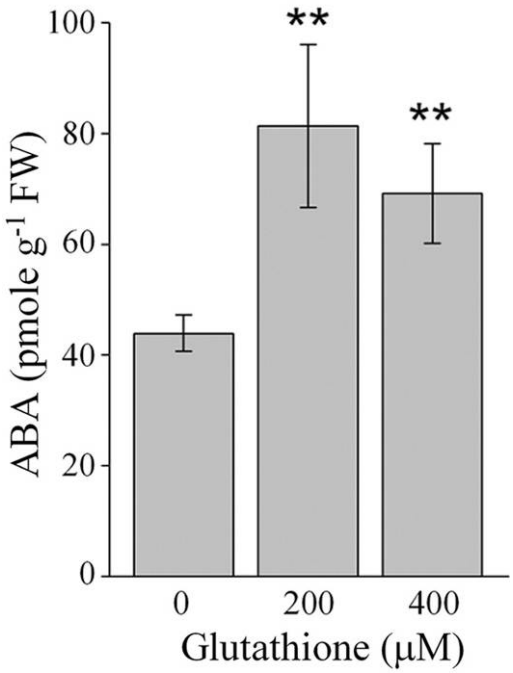

Figure 15. Effect of exogenous GSH on ABA accumulation in leaf tissues.

Col-0 were grown in water containing GSH (200 and 400 μM) in a growth chamber of 22 ^{o}C under 16-h light/ 8-h dark conditions. ABA levels were determined using 3-week-old plants. Values represent the means ± standard deviation (SD) from three samples. Three independent experiments were performed with similar results. Three independent experiments were performed with the same trends. Error bars represent the standard deviation (SD) (*t* test; **, $p < 0.01$).

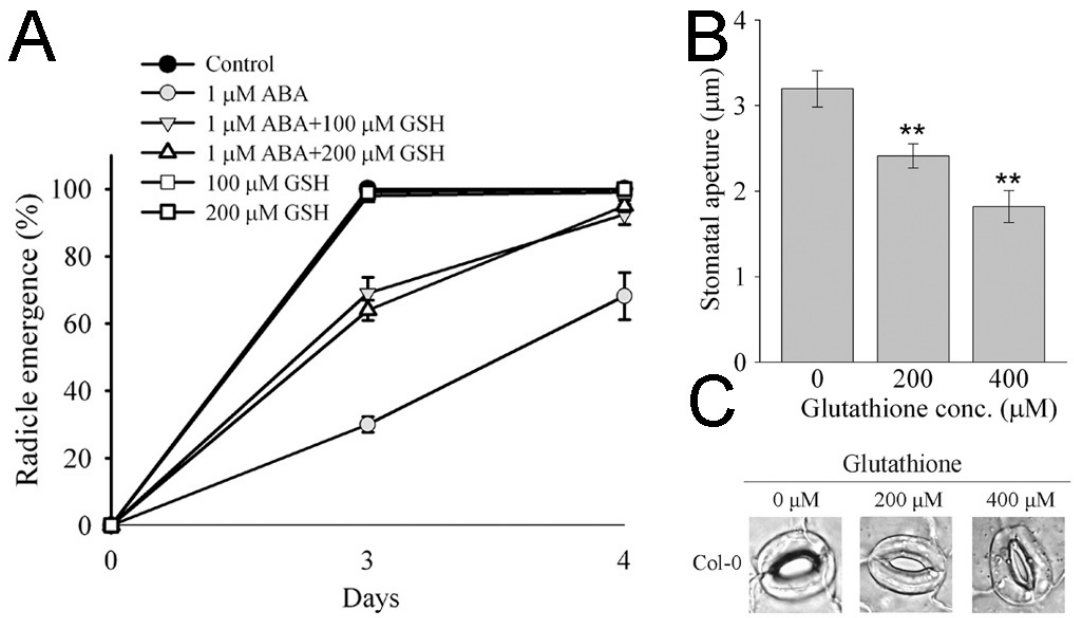

Figure 16. Effect of exogenous GSH and ABA on seed germination and stomata aperture.

(A) GSH reduced seed germination sensitivity to ABA inhibition. Col-0 seeds were germinated and grown on 1/2 MS agar plates containing ABA or GSH for 4 days. Data are presented as the means ±standard deviation (SD). Five independent experiments were performed with similar result.

(B) GSH reduced the intrinsic stomata aperture size. Leaves of 5-week-old Col-0 plants growing in the water solution containing indicated concentration of GSH were peeled and floated on water under light for 2.5 h, and stomatal apertures were measured. Values are the means and SD ($n > 60$). **Significantly differs from the Col-0 ($p < 0.01$), by Student's *t*-test. These experiments were repeated at least three times.

(C) Micrographs representing the dynamics of GSH-mediated stomatal closure in B.

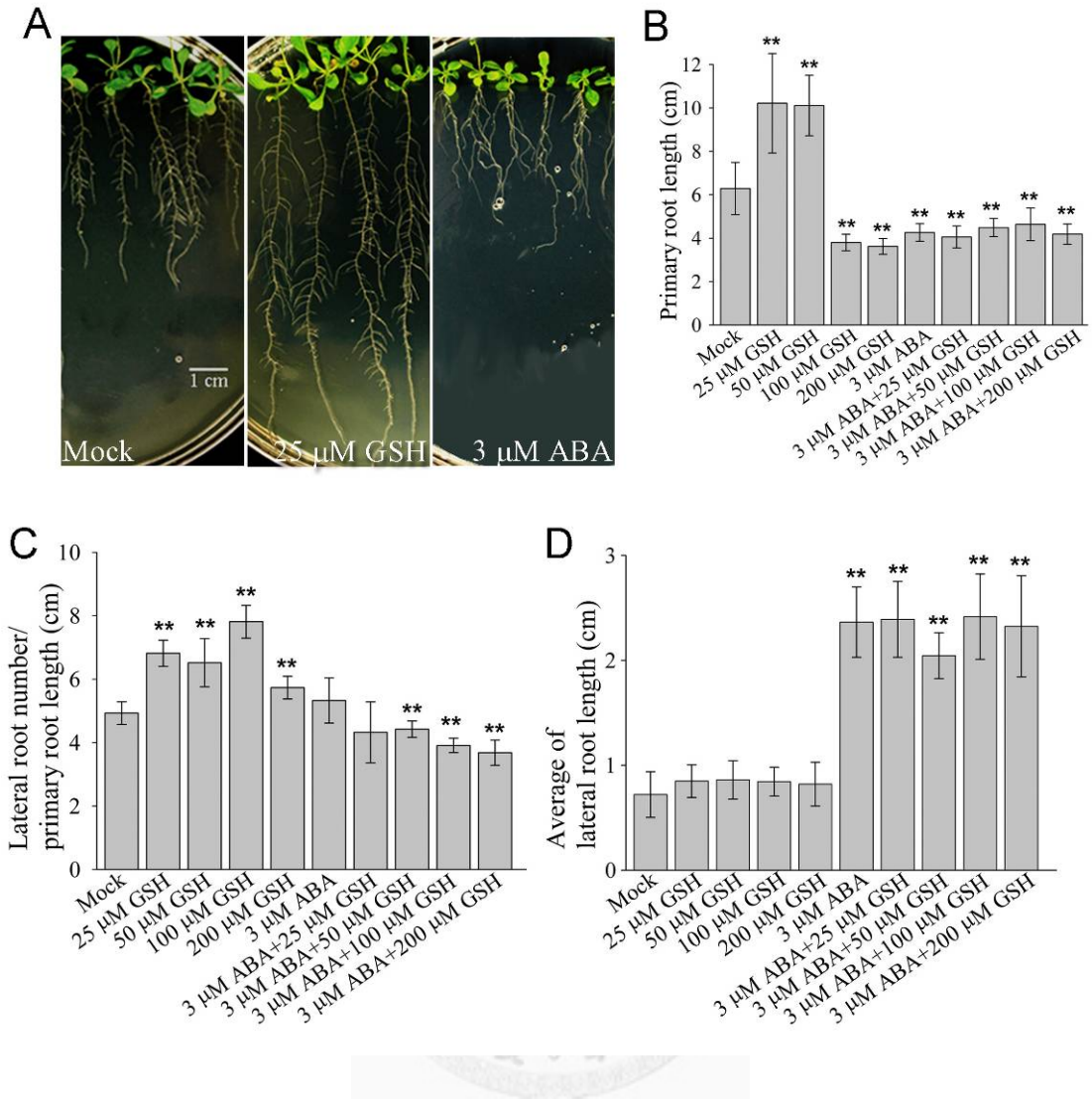

Figure 17. Effect of exogenous GSH, ABA on the root architecture.

(A) Image of seedlings of 2-week-old Col-0 plants growing in 1/2 MS agar plate (left), or supplemented with 25 μM GSH (central), or supplemented with 3 μM ABA (right).

(B) Comparison of the primary root length. Thirty plants at each condition were counted and averaged.

(C) Lateral root number per cm of primary root. Only lateral roots longer than 0.5 cm were used for the calculation.

(D) Average lateral root length.

Ten plants at each condition were counted and averaged for C and D. Error bars represent the standard deviation (SD) (*t* test; **, $p < 0.01$).

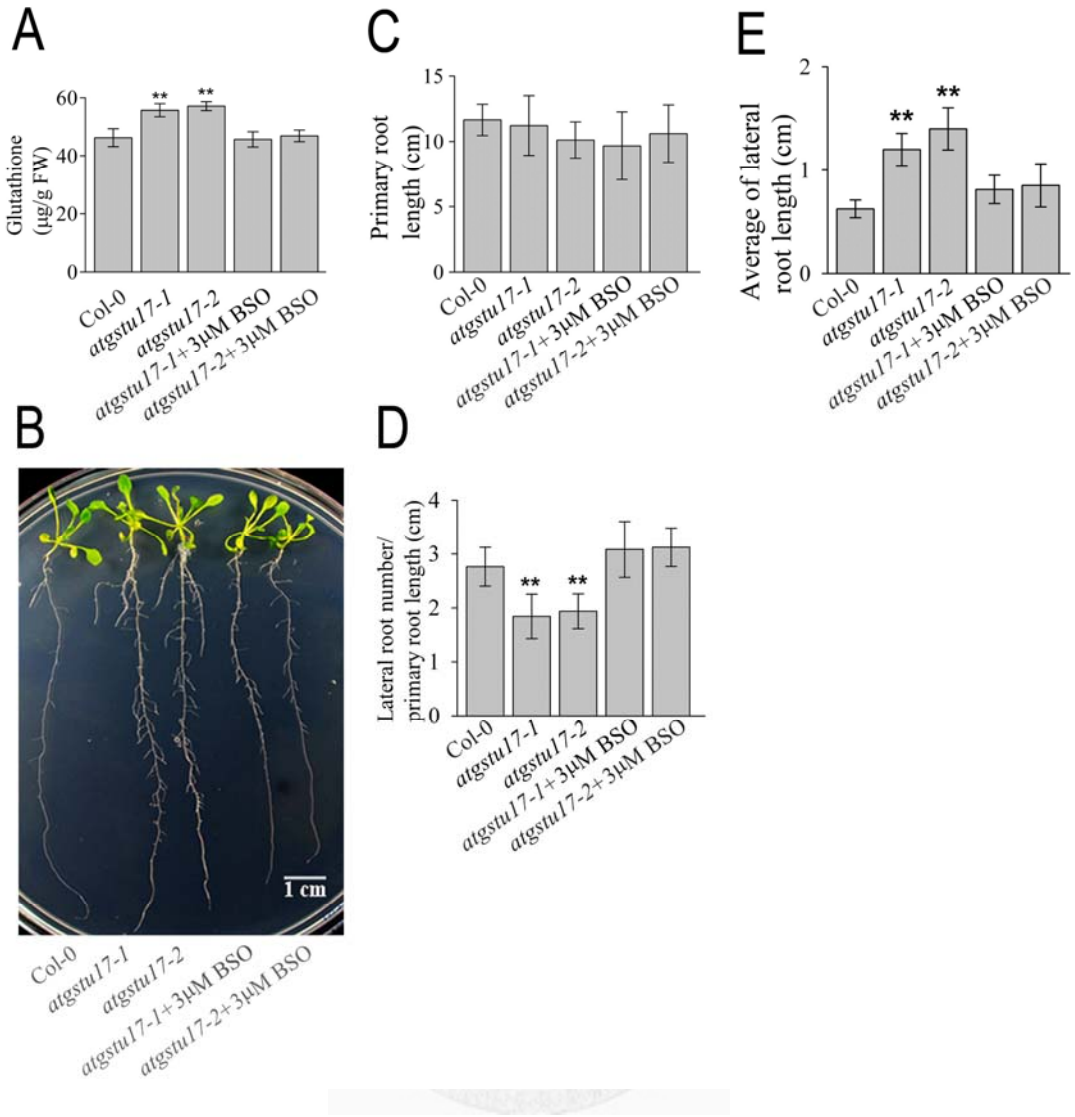

Figure 18. Effect of exogenous BSO on the root architecture.

(A) BSO treatment reduces GSH content of *atgstu17-1* and *atgstu17-2* leaves. Plants were grown under 16-h light/ 8-h dark conditions with or without BSO, and leaves of 2-week old plants were used for GSH assay. These experiments were repeated twice and gave comparable results.

(B) Image of seedlings of 2-week-old Col-0 and *atgstu17*-mutant plants growing in 1/2 MS agar plate with or absence of 3 μM BSO. For photograph purpose plants from separated plates were arranged side by side.

(C) Comparison of the primary root length. Thirty plants at each condition were

counted and averaged.

(D) Lateral root number per cm of primary root. Only lateral roots longer than 0.5 cm were used for the calculation.

(E) Average lateral root length.

Ten plants at each condition were counted and averaged for D and E. Error bars represent the standard deviation (SD) (*t* test; **, $p < 0.01$).

Figure 19. Effect of exogenous GSH and ABA on drought and salt tolerance.

Three-week-old Col-0 plants were incubated in water solution containing ABA, or GSH or different combinations of ABA and GSH at 22 ^{o}C under 16-h light/ 8-h dark conditions. Newly prepared solution was supplied every two days. Mock indicates plants growing in water solution only. Each treatment consisted of 3 pots with 20 plants in each pot. Five independent experiments were performed with similar results. Watering was stopped for 10 days and then resumed watering. The photographs were taken before re-watering. The survival rates after re-watering for 5 days were indicated (upper panel). Plants were watered for 12 days at 4-day intervals with increasing concentrations of NaCl of 100, 200, and 300 mM along with the ABA and GSH as indicated. The photographs were taken at 18 days incubation. The survivors were quantified as described for Fig. 4D (lower panel).

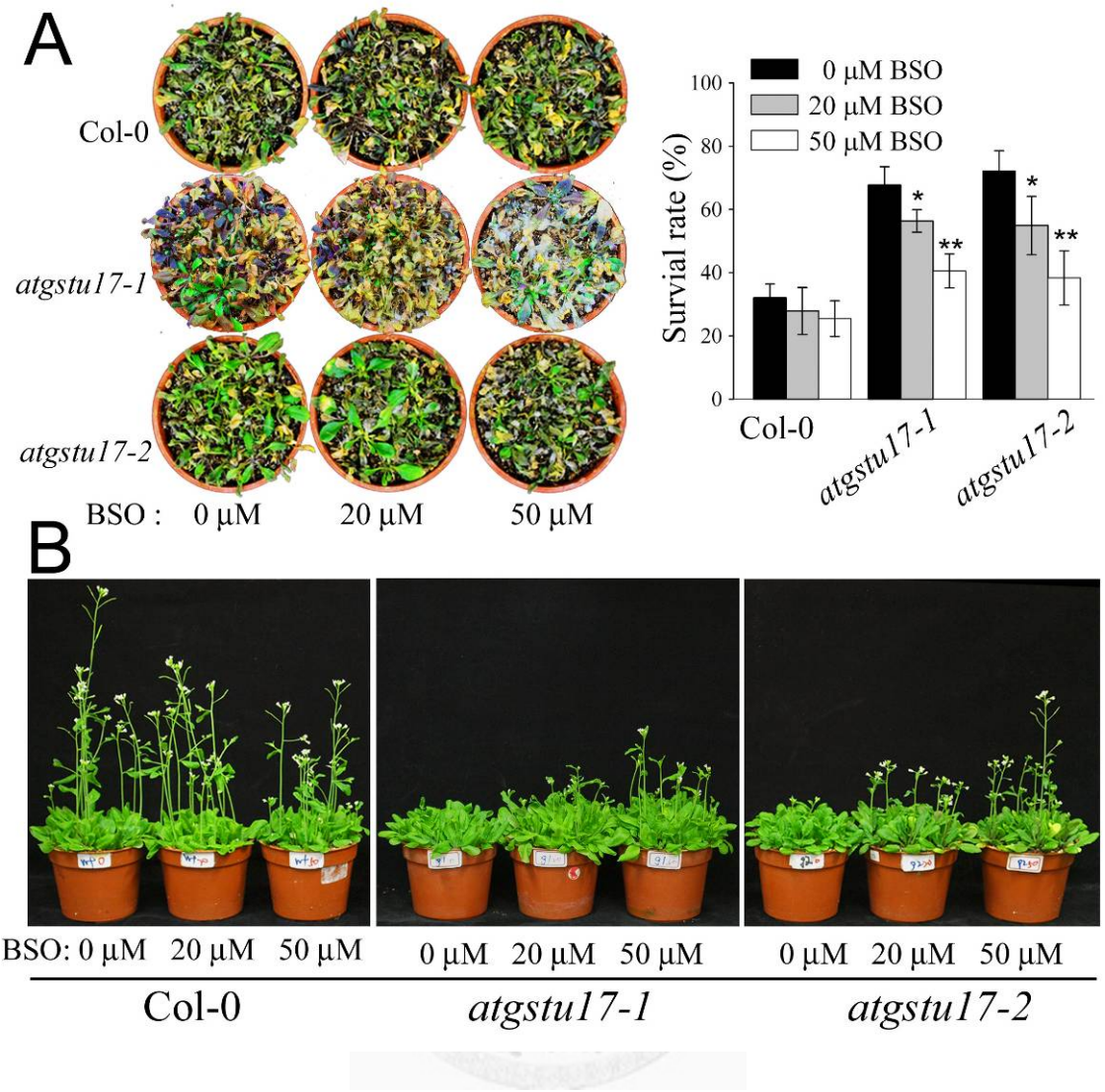

Figure 20. Drought tolerance test and flowering time of *atgstu17*-mutant and Col-0 plants grown in the solution with or without BSO.

(A) BSO treatment confers reduced tolerance of the *atgstu17-1* and *atgstu17-2* to short-term drought. Plants were grown under 16-h light/ 8-h dark conditions with or without BSO. Watering of 2-week-old plants was withdrawn for 10~12 days and then resumed watering. The photograph showing the differences in the reactions of plants to drought were taken after 5 days of re-watering. The survival rates (%) were calculated from the numbers of surviving plants per total plants tested. Data are presented as the means of 3 pots each treatment. Three

independent experiments were performed with similar results.

(B) BSO treatment reduces the bolting time of the *atgstu17*-mutant plant. Growth condition is same as A.

These experiments were repeated three times and gave comparable results.

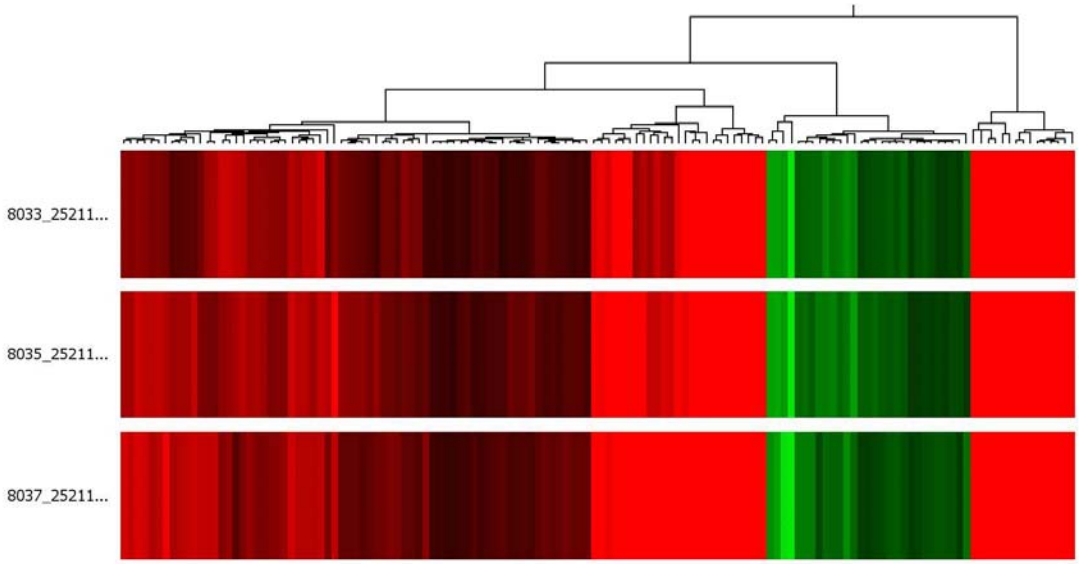

Figure 21. Clustered display of Gene expression from *atgstu17-2* microarray data.

Each experiment shows consistent expression profiling using Hierarchical Clustering.

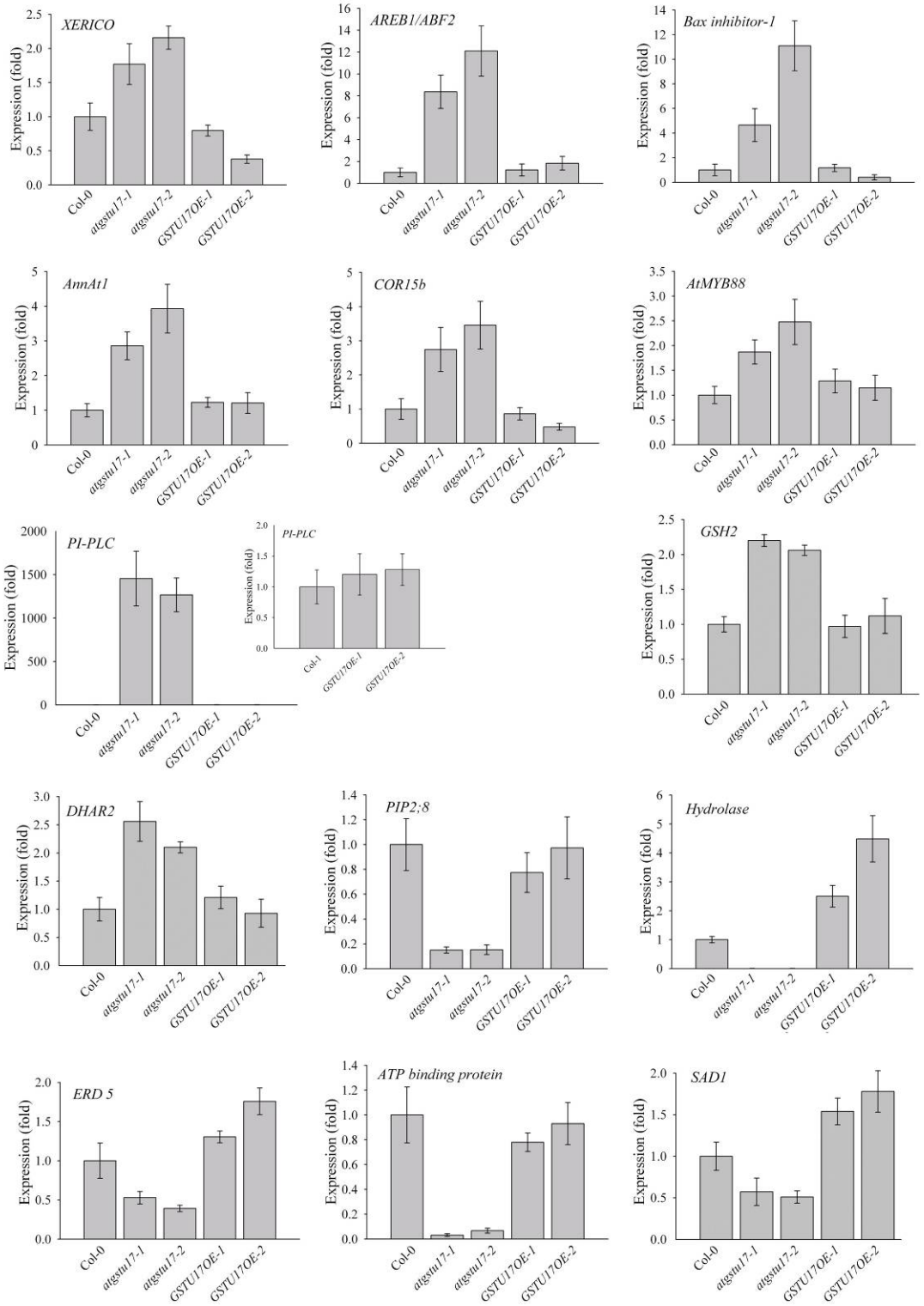

Figure 22. Expression of selected genes from the microarray dataset in the *AtGSTU17*-mutant lines and Col-0 plants.

RNAs were prepared from *atgstu17* mutants, *GSTU17OE* lines and Col-0 plants

under normal growth conditions that are described in Table S1. DNA primers for amplification of each specific gene are listed in the Supplemental Table S2. *XERICO* (At2g04240), *AREB1* (At1g45249), *PI-PLC* (At3g47290), *Bax inhibitor-1* (At5g47130), *AnnAt1* (At1g35720), *COR15b* (At2g42530), *GSH2*(At5g27380), *DHAR2*(At1g75270) and *AtMYB88* (At2g02820) were upregulated genes, while hydrolase (At1g66860), ATP-binding kinase protein (At1g51830), *ERD5* (At3g30775, proline dehydrogenase), *SAD1*(At5g48870) and *PIP2.8* (At2g16850) were downregulated genes. The amplification of *Actin8* was used as an internal control to normalize all data. The level of each gene transcript in the Col-0 was set to 1.0. Three independent experiments were performed with similar results.

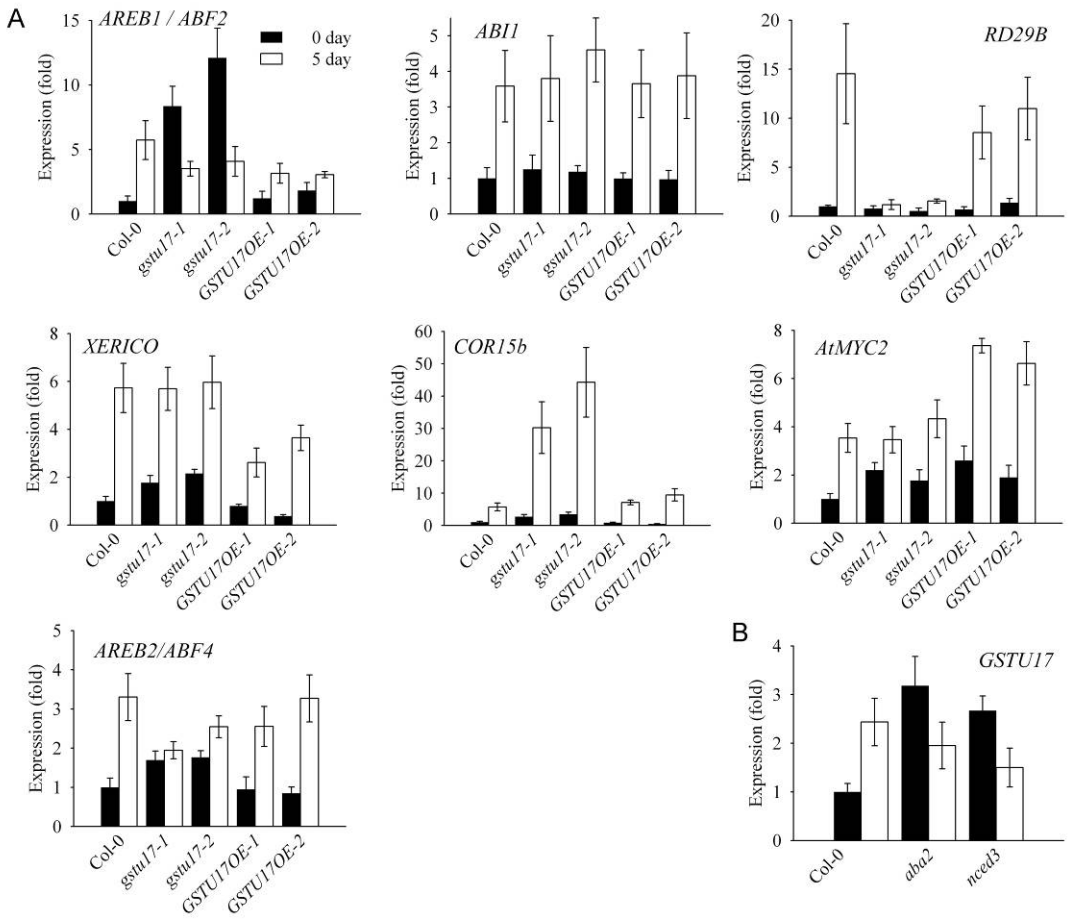

Figure 23. *AtGSTU17* regulating downstream gene expressions and *AtGSTU17* induction in ABA-deficient mutant plants.

(A) Real-time PCR assay of the accumulation of specific gene transcripts obtained from Col-0 plants and *AtGSTU17*-mutant lines by withholding water for 5 d from 3-week-old soil-grown plants grown in a growth chamber under 16-h light/8-h dark conditions.

(B) Real-time PCR assay of the expression of *AtGSTU17* obtained from Col-0 plants, and *aba2*- and *nced3*-mutant lines by withholding water for 5 d from 3-week-old soil-grown plants grown in a growth chamber under16-h light/8-h dark conditions.

Amplification of *Actin8* was used as an internal control to normalize all data. The

level of each gene transcript in the Col-0 before dehydration was set to 1.0. Three independent experiments were performed with similar results.

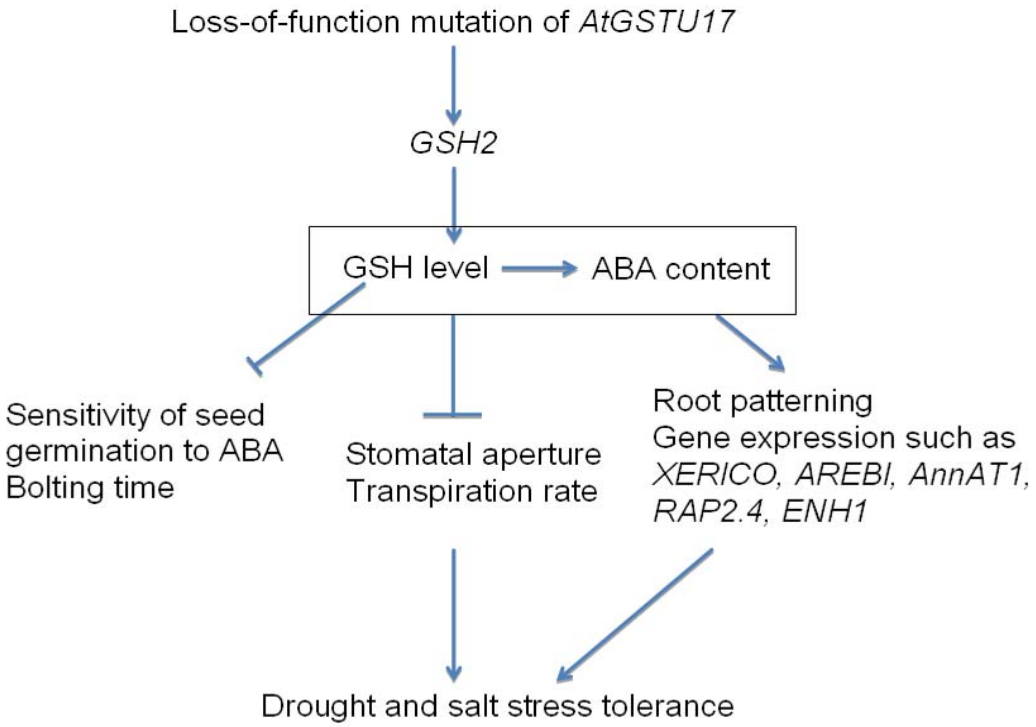

Figure 24. A model for the *atgstu17* modulation of drought and salt stress tolerance and other phenotypes.

The underlying mechanism linking loss-of-function mutation of the *ATGSTU17* with phenotypes is mainly because the accumulation of GSH in the *atgstu17* mutants which might associate with increased level of ABA in planta. Some of the phenotypes, i.e., sensitivity of seed germination to ABA and delayed flowering are specific to the GSH accumulation. Other phenotypes like, stomatal aperture, root architecture, gene expression, and drought and salt stress tolerance are resulting from the combined action of GSH and ABA.

APPDENDIX

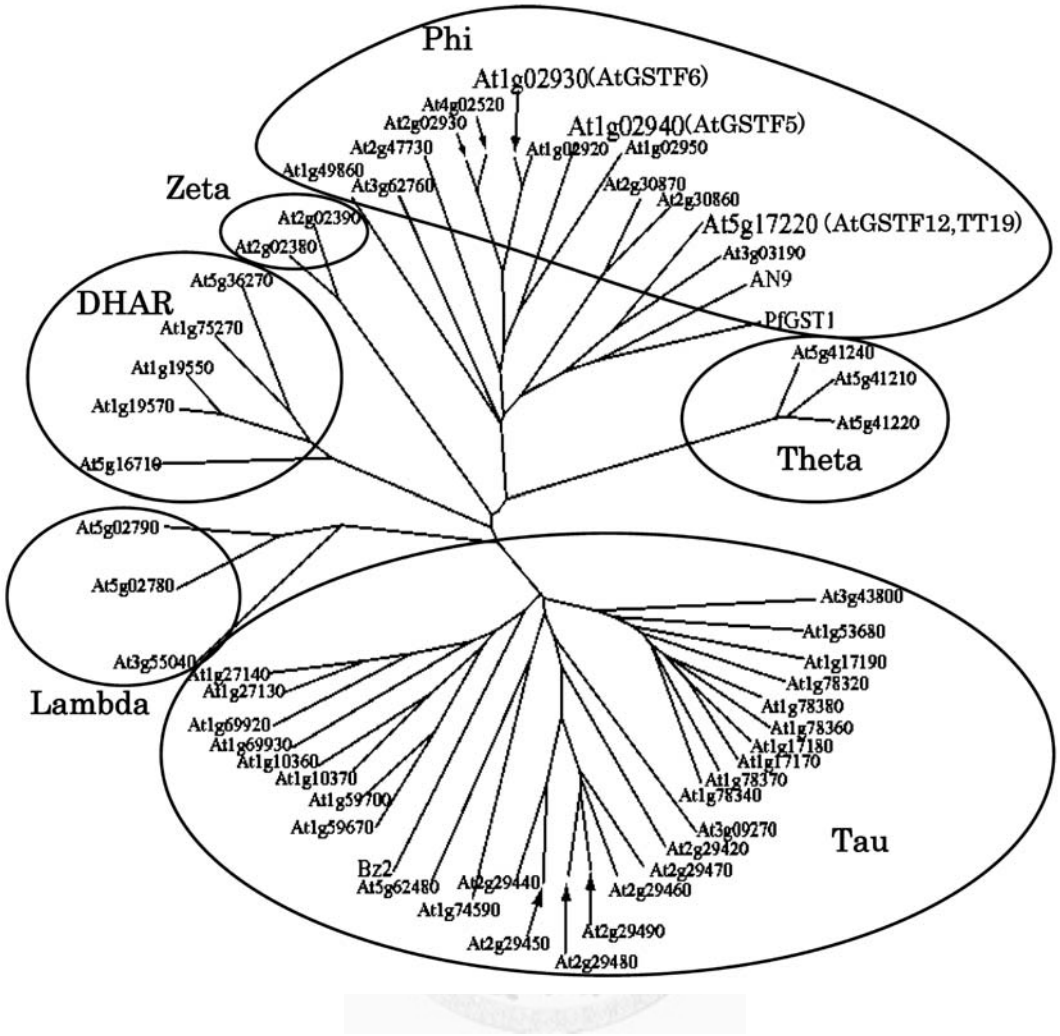

Supplemental Figure S1. Phylogenetic analysis of *Arabidopsis* GST homologues.

AtGSTU17 (At1g10370) encodes a glutathione S-transferase and belongs to the Tau class.

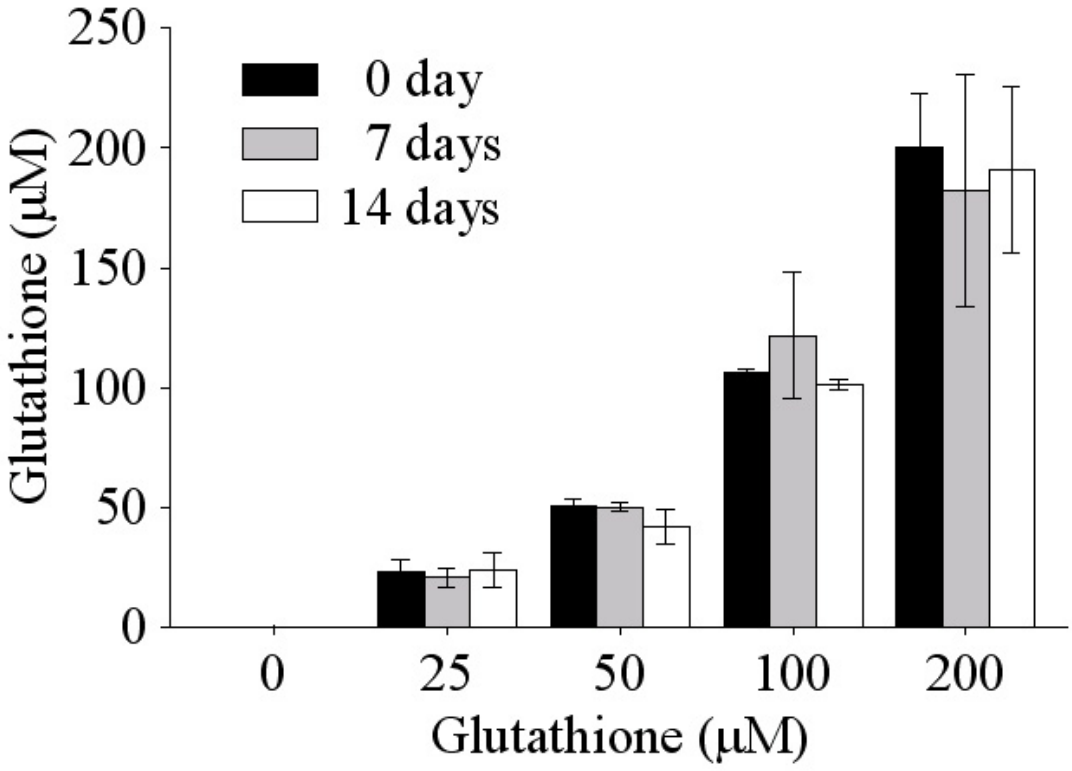

Supplemental Figure S2. The stability of exogenous GSH in the MS medium.

The half-strength MS medium containing indicated concentration of GSHs was incubated in a growth chamber at 22 °C under a 16-h light, 8-h dark photoperiod. The GSH content after incubation for 0, 7 and 14 days were measured. Glutathione reductase was omitted from the assay method. These experiments were repeated at least three times.

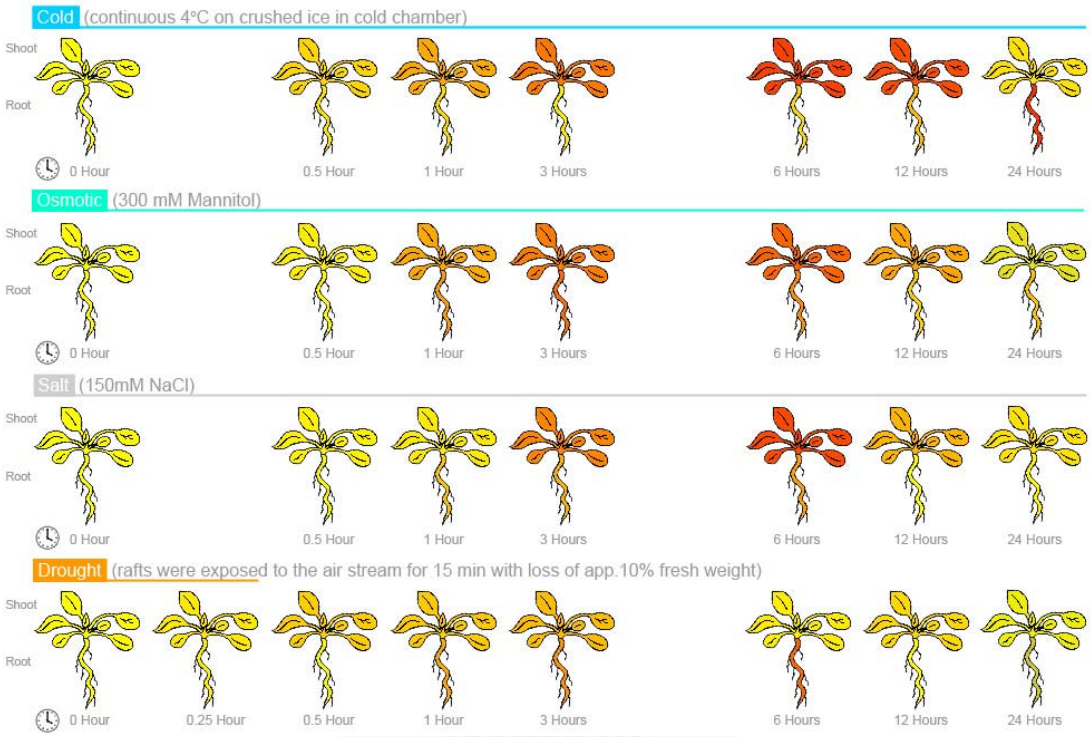

Supplemental Figure S3. Expression profile of *AtGSTU17* under various abiotic stresses according to Arabidopsis eFP Browser.

AtGSTU17 was induced by drought stress, salt stress, osmotic stress, cold and drought stress.

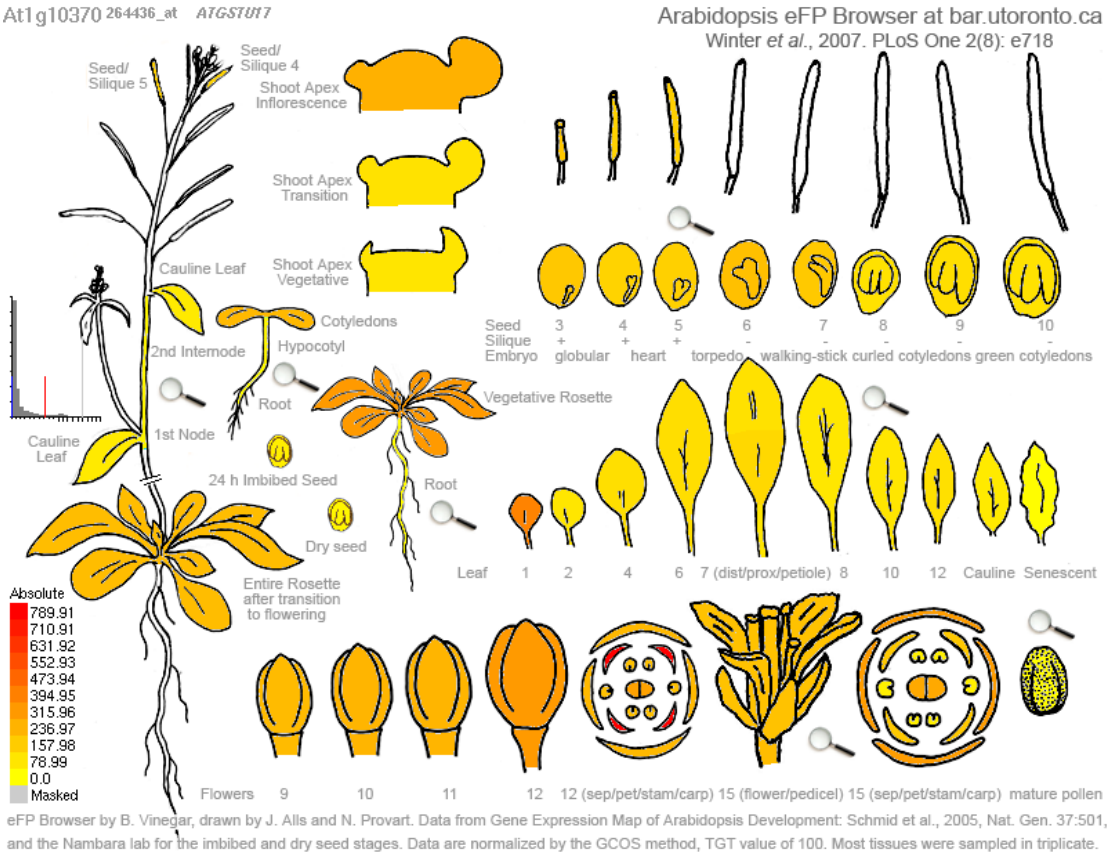

Supplemental Figure S4. Expression profile of *AtGSTU17* in different organs and tissues and stages based on Arabidopsis eFP Browser.

AtGSTU17 expressed in stems, leaves, and flowers, but has lower expression levels in root and matured siliques.

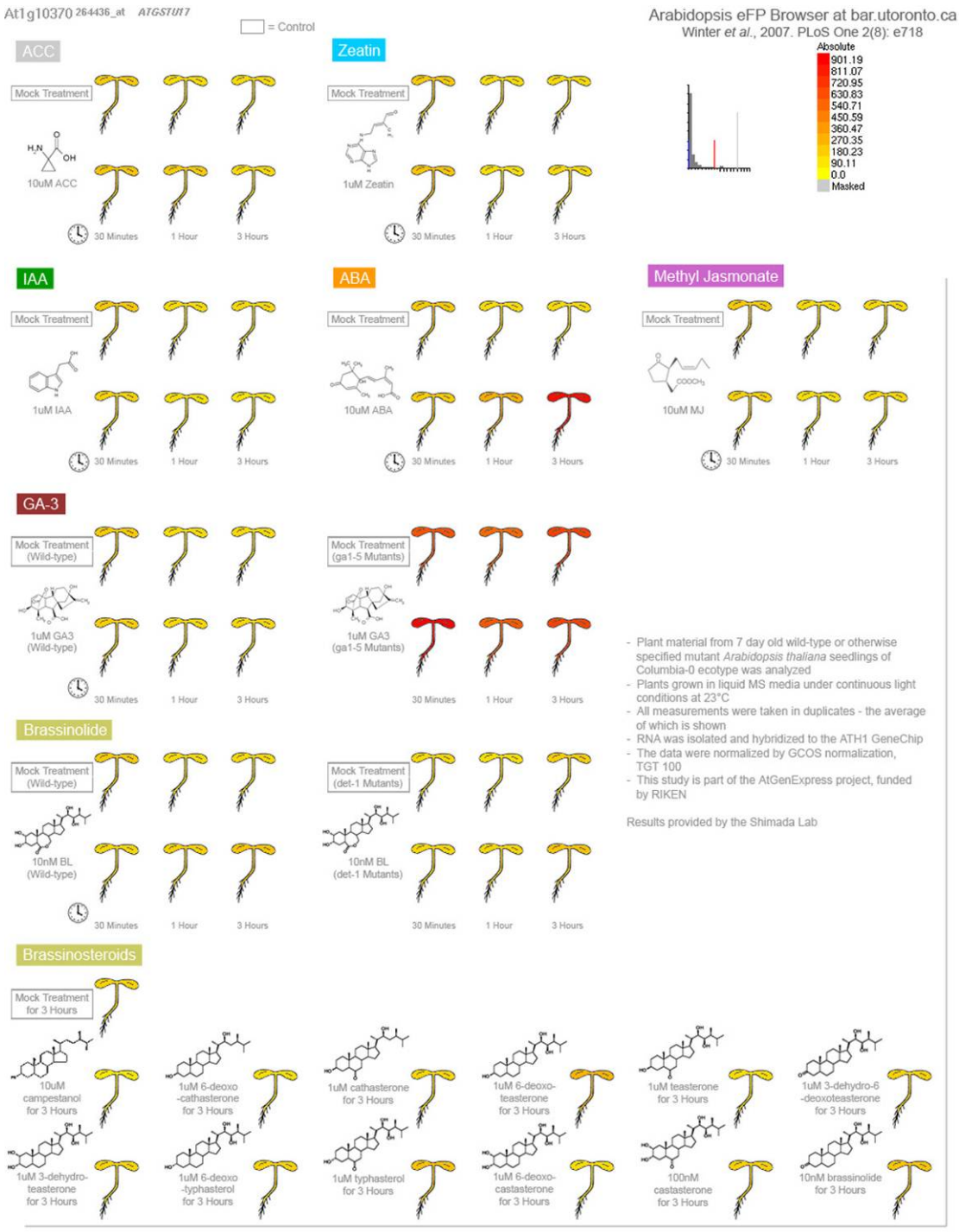

Supplemental Figure S5. Expression profile of *AtGSTU17* under various plant hormones according to Arabidopsis eFP Browser.

AtGSTU17 was induced by ABA.

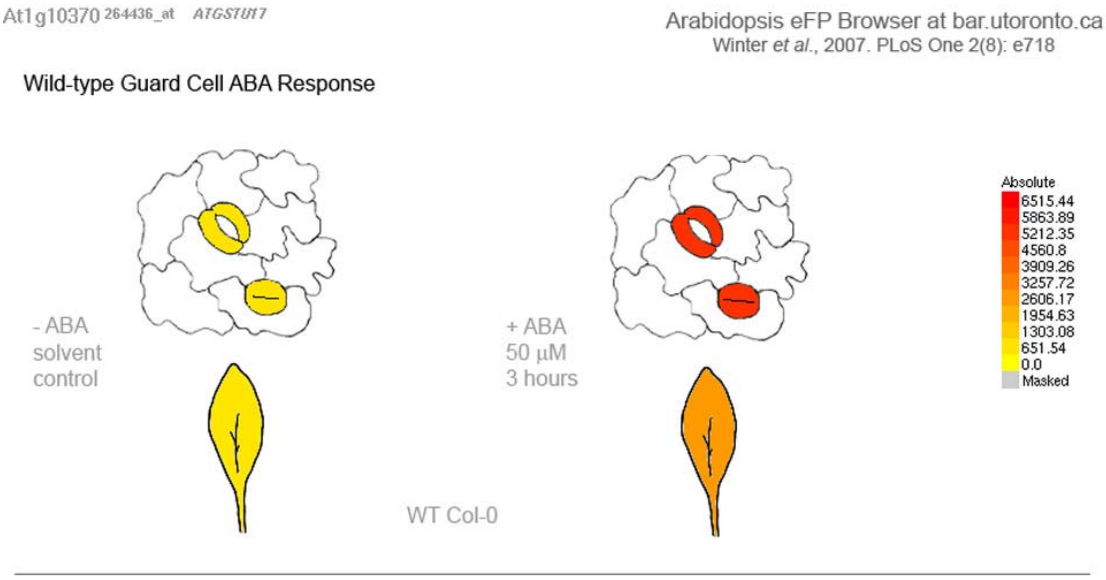

Supplemental Figure S6. *AtGSTU17* can be induced by ABA and expressed in guard cell based on Arabidopsis eFP Browser.

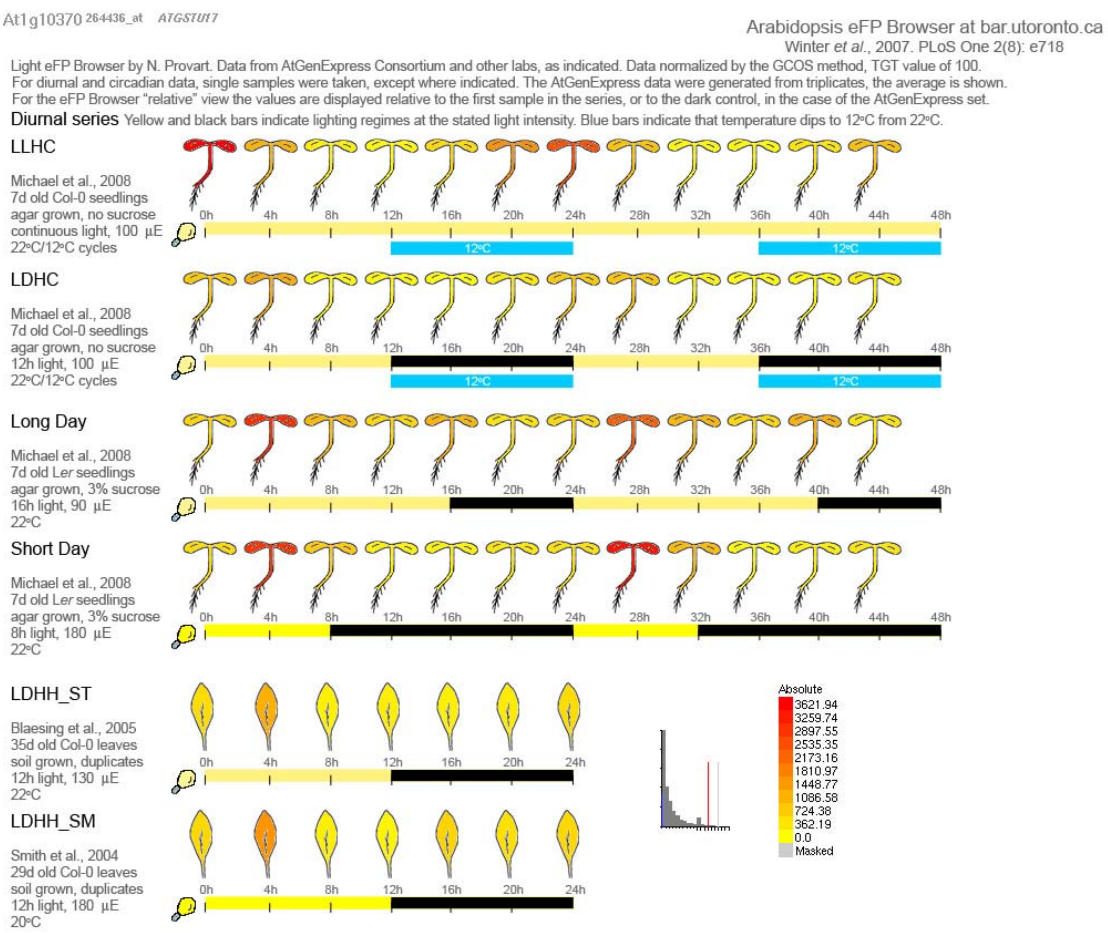

Supplemental Figure S7. The expression of *AtGSTU17* also shows a circadian rhythm based on Arabidopsis eFP Browser.

AtGSTU17 can be induced by Light in long-day or short-day condition.